Electronic Supporting Information

Fe(II) complexes of 2,2':6',2"-terpyridine ligands functionalized with substituted-phenyl groups: Synthesis, crystal structures and anticancer potential

Dameng Sun,[a] Xin Huang,[a] Ruojun Man, [b] Xinjie Jia,[a] Xinluan Song,[a] Sihan Wang,[a] Xingyong Xue, *[b] Hongming Liu,*[a] and Zhen Ma*[a]

[a] School of Chemistry and Chemical Engineering, Guangxi University, 530004 Nanning, Guangxi, People's Republic of China. E-mail: hongming9224@126.com(H. Liu), mzmz2009@sohu.com(Z. Ma).
[b] School of Chemistry and Chemical Engineering, Guangxi Minzu University, 530006 Nanning, Guangxi, People's Republic of China. E-mail: 315254042@qq.com(X. Xue).

Index

Figure S1 The IR spectrum of complex **1** 3
Figure S2 The IR spectrum of complex **2** 3
Figure S3 The IR spectrum of complex **3** 4
Figure S4 The IR spectrum of complex **4** 4
Figure S5 The IR spectrum of complex **5** 5
Figure S6 The IR spectrum of complex **6** 5
Figure S7 The IR spectrum of complex **7** 6
Figure S8 The IR spectrum of complex **8** 6
Figure S9 The IR spectrum of complex **9** 7
Figure S10 The ESI-MS spectrum of complex **1** 7
Figure S11 The ESI-MS spectrum of complex **2** 8
Figure S12 The ESI-MS spectrum of complex **3** 8
Figure S13 The ESI-MS spectrum of complex **4** 9
Figure S14 The ESI-MS spectrum of complex **5** 9
Figure S15 The ESI-MS spectrum of complex **6** 10
Figure S16 The ESI-MS spectrum of complex **7** 10
Figure S17 The ESI-MS spectrum of complex **8** 11
Figure S18 The ESI-MS spectrum of complex **9** 11
Figure S19 Stacking diagram of complexes **1-5** structure 12
Figure S20 Fe2p XPS spectra of complexes **1-2** 12
Figure S21 XPS survey scan of complexes **1**(a) and **2**(b) 12
Figure. S22 The microscopic images of SiHa cells after treating with complexes **1-9** and cisplatin 14
Figure. S23 The microscopic images of Bel-7402 cells after treating with complexes **1-9** and

cisplatin 16
Figure. S24 The microscopic images of Eca-109 cells after treating with complexes **1-9** and cisplatin 18
Figure. S25 The microscopic images of HL-7702 cells after treating with complexes **1-9** and cisplatin 20
Figure. S26 UV spectra of complexes **1-9** in Tris-HCl buffer (pH 7.2) recorded at different times (within 24 h) at room temperature 21
Figure S27 Absorption spectra of 15 μM of complexes **1-2**(a-b) and **4-9**(c-h) in a Tris-HCl buffer (pH = 7.2) solution with series concentrations of CT-DNA. The plots of $A_0/(A-A_0)$ versus the concentration of CT-DNA are shown as the insets 22
Figure S28 CD spectra of complexes **1-2**(a-b) and **4-9**(c-h) to CT-DNA at different concentration ratios 23
Figure S29 The most favorable conformation of complex **2** bound with oligonucleotide (4JD8) .24
Figure S30 The most favorable conformation of complex **3** bound with oligonucleotide (4JD8) .24
Figure S31 The most favorable conformation of complex **4** bound with oligonucleotide (4JD8) .25
Figure S32 The most favorable conformation of complex **5** bound with oligonucleotide (4JD8) .25
Figure S33 The most favorable conformation of complex **1** bound with DNA-Topo I (1SC7) 26
Figure S34 The most favorable conformation of complex **2** bound with DNA-Topo I (1SC7) 26
Figure S35 The most favorable conformation of complex **4** bound with DNA-Topo I (1SC7) 27
Figure S36 The most favorable conformation of complex **5** bound with DNA-Topo I (1SC7) 27
Figure S37 The most favorable conformation of complex **1** bound with BSA (4F5S) 28
Figure S38 The most favorable conformation of complex **2** bound with BSA (4F5S) 28
Figure S39 The most favorable conformation of complex **4** bound with BSA (4F5S) 29
Figure S40 The most favorable conformation of complex **5** bound with BSA (4F5S) 29
Figure S41 Fluorescence spectra of 20 μM BSA in the absence (dotted line) and presence (2-20 μM) of complexes **1-2**(a-b) and **4-9**(c-h) (solid line) 30
Figure S42 CD spectra of complexes **1-2**(a-b) and **4-9**(c-h) to BSA at different concentration ratios 31
Table S1 Percentage of element content measured in XPS 32

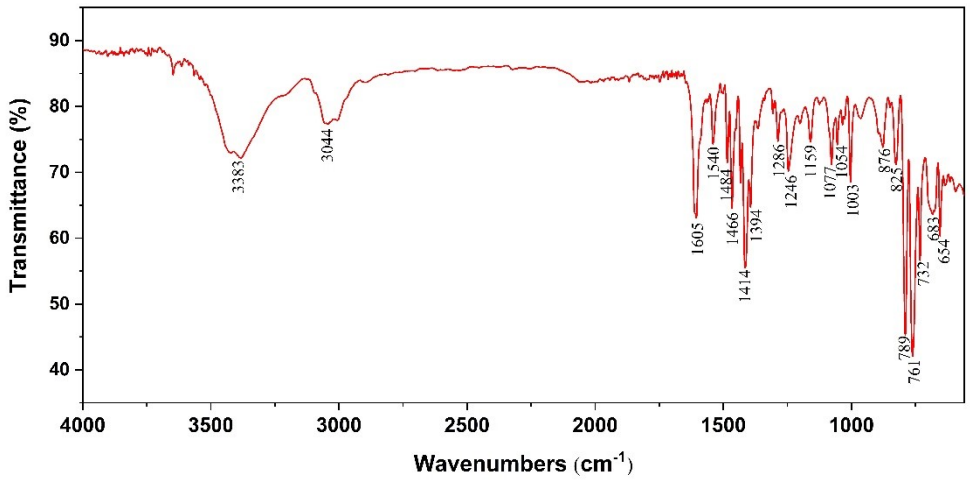

Figure S1 The IR spectrum of complex **1**

[$FeBr_2$**L**$_2$[1]] (**1**): IR (KBr, cm^{-1}): 3383 (m, υ_{O-H}), 3044 (m, υ_{C-H}), 1605 (s, $\upsilon_{C=C}$), 1540 (m, $\upsilon_{C=C}$), 1484 (m, $\upsilon_{C=C}$), 1466 (m, $\upsilon_{C=C}$), 1414 (s, $\upsilon_{C=C}$), 1394(m, $\upsilon_{C=C}$), 1286 (w, β_{C-H}), 1246 (m, β_{C-H}), 1159 (m, β_{C-H}), 1077 (m, β_{C-H}), 1054 (w, β_{C-H}), 1003 (m, β_{C-H}), 876 (m, γ_{C-H}), 825 (m, γ_{C-H}), 789 (s, γ_{C-H}), 761 (s, γ_{C-H}), 732 (m, γ_{C-H}), 683 (w, γ_{C-H}), 654 (m). Elemental analysis: Anal. calcd for $C_{42}H_{32}N_6Br_2Fe\cdot1.3HBr$:C, 53.39; H, 3.36; N, 8.94, Found: C, 53.58; H, 3.77; N, 9.01.

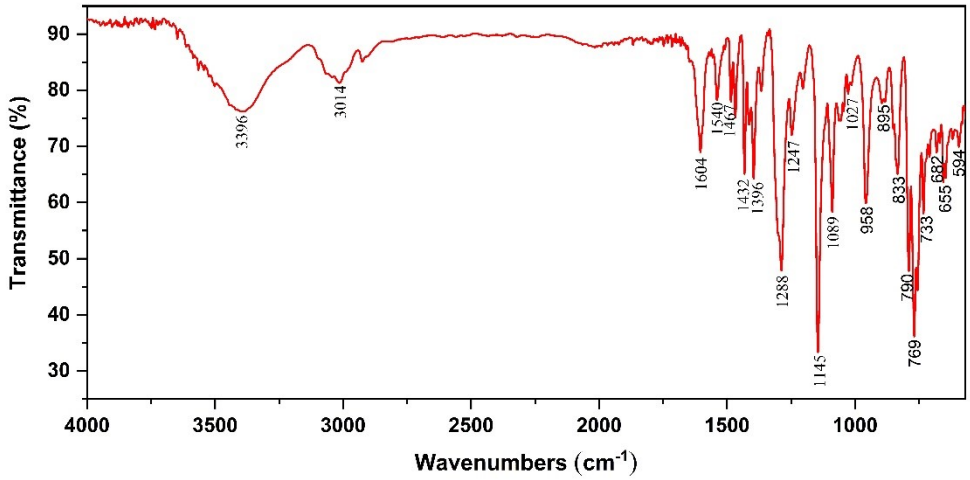

Figure S2 The IR spectrum of complex **2**

[$FeBr_2$**L**$_2$[2]] (**2**): IR (KBr, cm^{-1}): 3396 (m, υ_{O-H}), 3014 (m, υ_{C-H}), 1604 (m, $\upsilon_{C=C}$), 1540 (m, $\upsilon_{C=C}$), 1467 (m, $\upsilon_{C=C}$), 1432 (m, $\upsilon_{C=C}$), 1396 (m, $\upsilon_{C=C}$), 1288 (s, υ_{SO2}), 1247 (m, β_{C-H}), 1145 (s, υ_{SO2}), 1089 (m, β_{C-H}), 1027 (m, β_{C-H}), 958 (m), 895 (m, γ_{C-H}), 833 (m, γ_{C-H}), 790 (m, γ_{C-H}), 769 (s, υ_{SO2}), 733 (m, γ_{C-H}), 682 (w, γ_{C-H}), 655 (m), 646 (m), 553 (s, δ_{SO2}). Elemental analysis: Anal. calcd for $C_{44}H_{34}O_4S_2N_6Br_2Fe\cdot4H_2O$:C, 49.73; H, 3.98; N, 7.91, Found: C, 49.41; H, 4.00; N, 7.84.

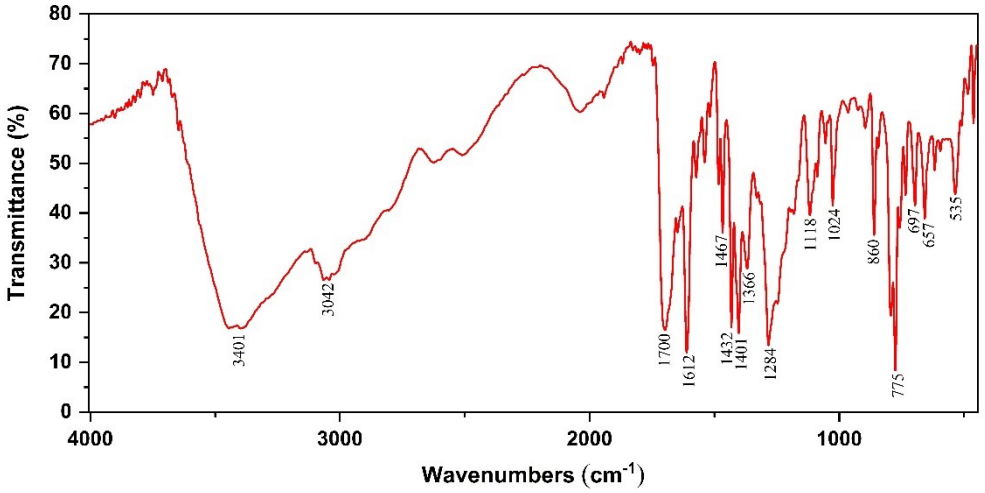

Figure S3 The IR spectrum of complex **3**

[$FeBr_2$**L**$_2$[3]] (**3**): IR (KBr, cm^{-1}): 3401 (m, υ_{O-H}), 3042 (m, υ_{C-H})), 1700 (s, $\upsilon_{C=O}$), 1612 (s, $\upsilon_{C=C}$), 1467 (m, $\upsilon_{C=C}$), 1432 (s, $\upsilon_{C=C}$), 1401 (s, $\upsilon_{C=C}$), 1366 (m, υ_{C-O}), 1284 (s, υ_{C-O}), 1118 (m, β_{C-H}), 1024 (m, β_{C-H}), 860 (m, γ_{C-H}), 775 (s, γ_{C-H}), 697 (m, γ_{C-H}), 657 (m), 535 (m).Elemental analysis: Anal. calcd for $C_{44}H_{30}O_4N_6Br_2Fe\cdot 6H_2O$:C, 51.28; H, 4.11; N, 8.16, Found: C, 51.05; H, 3.82; N, 8.14.

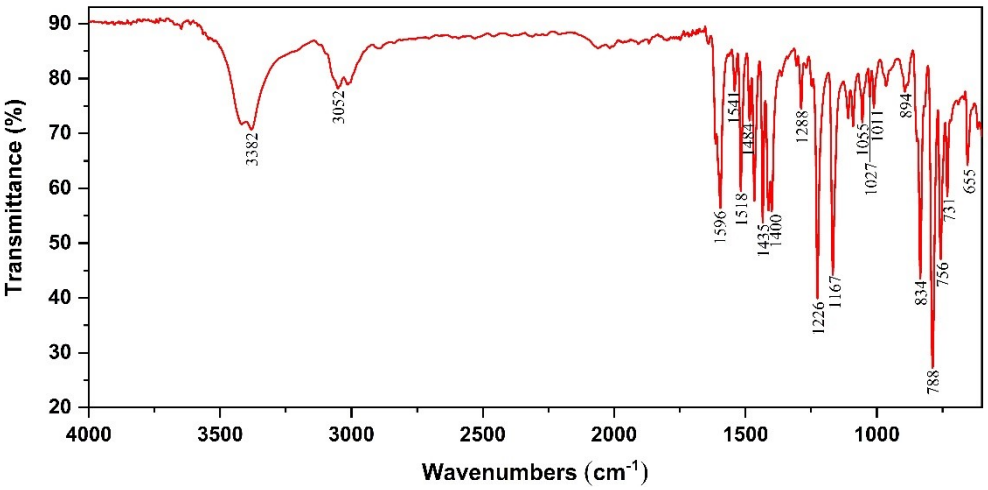

Figure S4 The IR spectrum of complex **4**

[$FeBr_2$**L**$_2$[4]] (**4**): IR (KBr, cm^{-1}): 3382 (m, υ_{O-H}), 3052 (m, υ_{C-H}), 1596 (m, $\upsilon_{C=C}$), 1541 (w, $\upsilon_{C=C}$), 1518 (m, $\upsilon_{C=C}$), 1484 (w, $\upsilon_{C=C}$), 1435 (m, $\upsilon_{C=C}$), 1400 (m), 1288 (m, β_{C-H}), 1226 (s, υ_{C-F}), 1167 (s, β_{C-H}), 1109 (m, β_{C-H}), 1055 (m, β_{C-H}), 1027 (m, β_{C-H}), 1011 (m, β_{C-H}), 894 (w, γ_{C-H}), 834 (s, γ_{C-H}), 788 (s, γ_{C-H}), 756 (s, γ_{C-H}), 731 (m, γ_{C-H}), 655 (m). Elemental analysis: Anal. calcd for $C_{42}H_{28}N_6F_2Br_2Fe\cdot 4H_2O$:C, 53.53; H, 3.85; N, 8.92, Found: C, 53.72; H, 3.45; N, 9.13.

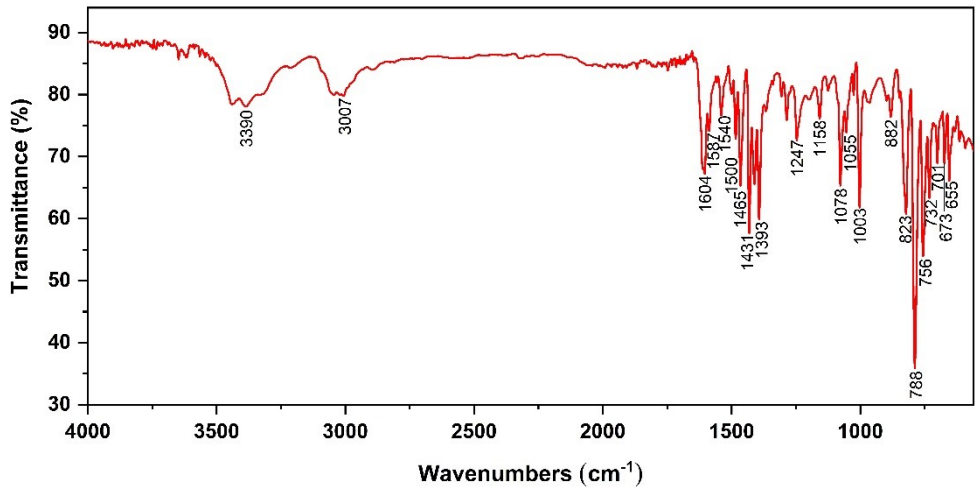

Figure S5 The IR spectrum of complex **5**

[$FeBr_2$**L**$_2^5$] (**5**): IR (KBr, cm^{-1}): 3390 (m, υ_{O-H}), 3007 (m, υ_{C-H}), 1604 (m, $\upsilon_{C=C}$), 1587 (m, $\upsilon_{C=C}$), 1540 (m, $\upsilon_{C=C}$), 1500 (w, $\upsilon_{C=C}$), 1465 (m, $\upsilon_{C=C}$), 1431 (s, $\upsilon_{C=C}$), 1393 (s, $\upsilon_{C=C}$) 1247 (m, β_{C-H}), 1158 (m, β_{C-H}), 1077 (m, β_{C-H}), 1055 (m, β_{C-H}), 1026 (w, β_{C-H}), 1003 (s, β_{C-H}), 882 (w, γ_{C-H}), 823 (m, γ_{C-H}), 788 (s, γ_{C-H}), 756 (s, γ_{C-H}), 731 (m, γ_{C-H}), 701 (m, γ_{C-H}), 673, 655 (m, γ_{C-Br}). Elemental analysis: Anal. calcd for $C_{42}H_{28}N_6Br_4Fe\cdot 4H_2O$:C, 47.40; H, 3.41; N, 7.90, Found: C, 47.51; H, 3.22; N, 7.98.

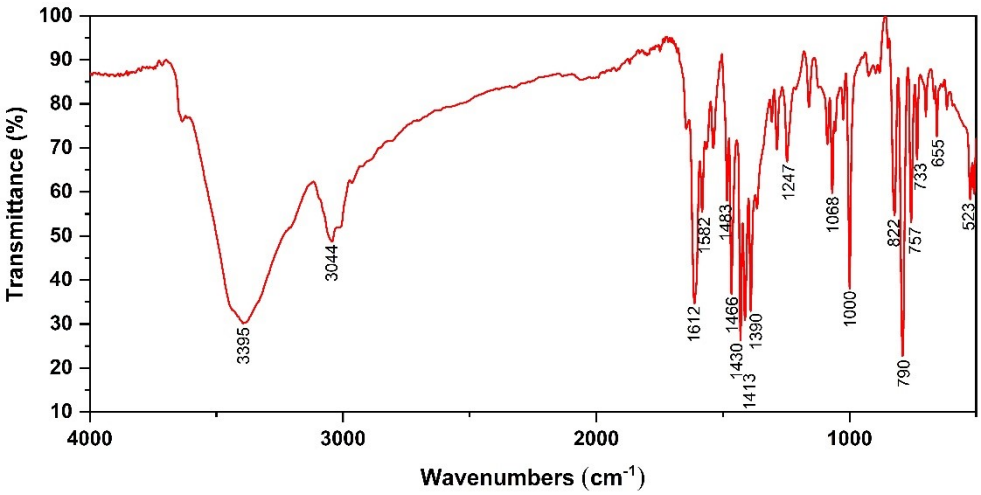

Figure S6 The IR spectrum of complex **6**

[$FeBr_2$**L**$_2^6$] (**6**): IR (KBr, cm^{-1}): 3395 (m, υ_{O-H}), 3044 (m, υ_{C-H}), 1612 (s, $\upsilon_{C=C}$), 1582 (m, $\upsilon_{C=C}$), 1483 (m, $\upsilon_{C=C}$), 1446 (s, $\upsilon_{C=C}$), 1430 (s, $\upsilon_{C=C}$), 1413 (s, $\upsilon_{C=C}$) 1390 (s), 1247 (m, β_{C-H}), 1068 (m, β_{C-H}), 1000 (m, β_{C-H}), 822 (m, γ_{C-H}), 790 (s, γ_{C-H}), 757 (m, γ_{C-H}), 733 (m, γ_{C-H}), 655 (m), 523 (m, γ_{C-I}). Elemental analysis: Anal. calcd for $C_{42}H_{28}N_6Br_2I_2Fe\cdot 5H_2O$:C, 42.89; H, 3.26; N, 7.14, Found: C, 42.41; H, 3.27; N, 7.02.

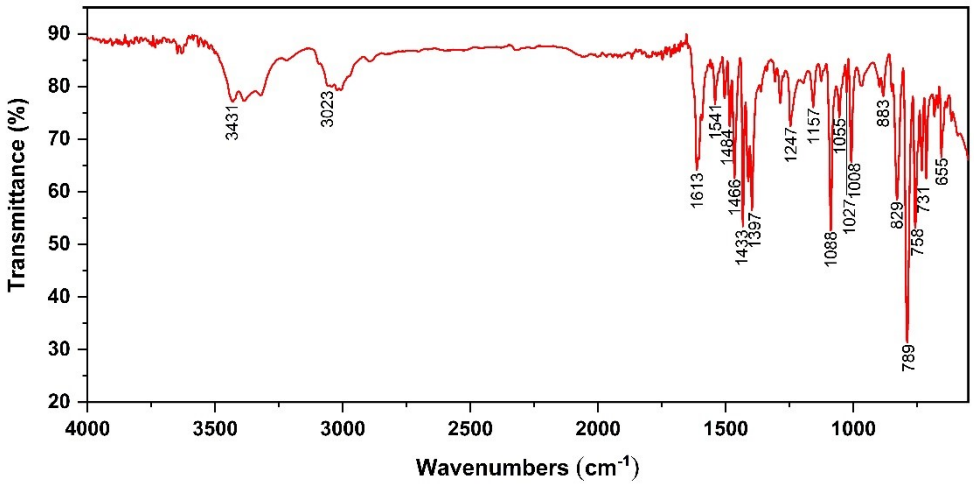

Figure S7 The IR spectrum of complex **7**

[$FeBr_2$**L**$_2$[7]] (**7**): IR (KBr, cm^{-1}): 3431 (m, υ_{O-H}), 3023 (m, υ_{C-H}), 1613 (m, $\upsilon_{C=C}$), 1541 (m, $\upsilon_{C=C}$), 1484 (m, $\upsilon_{C=C}$), 1466 (m, $\upsilon_{C=C}$), 1433 (s, $\upsilon_{C=C}$), 1397 (m), 1247 (m, β_{C-H}), 1157 (m, β_{C-H}), 1088 (s, β_{C-H}), 1054 (m, β_{C-H}), 1026 (w, β_{C-H}), 1008 (m, β_{C-H}), 883 (m, γ_{C-H}), 829 (s, γ_{C-H}), 789 (s, γ_{C-H}), 758 (m, γ_{C-H}), 731 (m, γ_{C-Cl}), 655 (m). Elemental analysis: Anal. calcd for $C_{42}H_{28}N_6Cl_2Br_2Fe\cdot 3H_2O$:C, 52.69; H, 3.58; N, 8.78, Found: C, 52.78; H, 3.64; N, 8.85.

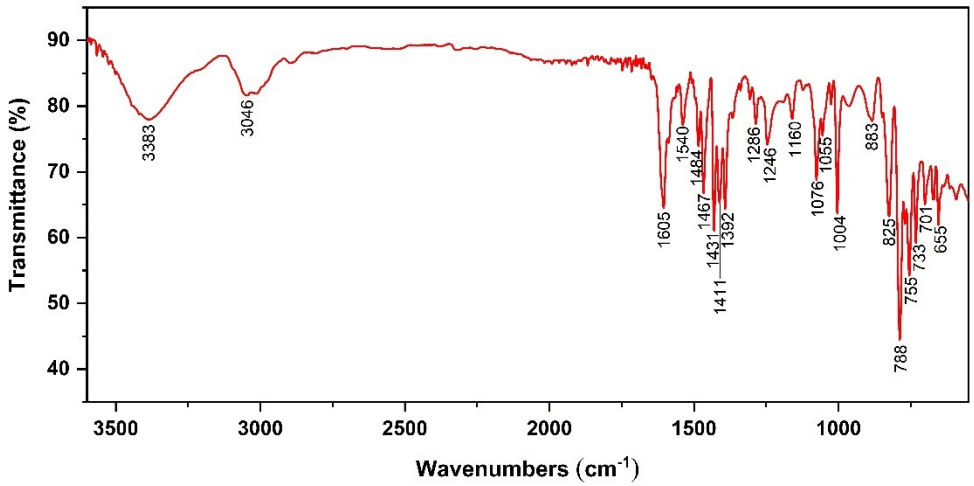

Figure S8 The IR spectrum of complex **8**

[$FeBr_2$**L**$_2$[8]] (**8**): IR (KBr, cm^{-1}): 3383 (m, υ_{O-H}), 3046 (m, υ_{C-H}), 1605 (s, $\upsilon_{C=C}$), 1540 (m, $\upsilon_{C=C}$), 1484 (m, $\upsilon_{C=C}$), 1466 (m, $\upsilon_{C=C}$), 1431 (s, $\upsilon_{C=C}$), 1411 (m, $\upsilon_{C=C}$), 1392 (m, $\upsilon_{C=C}$), 1286 (w, β_{C-H}), 1246 (m, β_{C-H}), 1160 (w, β_{C-H}), 1076 (m, β_{C-H}), 1055 (w, β_{C-H}), 1004 (s, β_{C-H}), 883 (m, γ_{C-H}), 825 (s, γ_{C-H}), 788 (s, γ_{C-H}), 755 (m, γ_{C-H}), 733 (m, γ_{C-H}), 701 (m), 655 (m). Elemental analysis: Anal. calcd for $C_{54}H_{38}N_6Br_2Fe\cdot 8H_2O$:C, 57.36; H, 4.81; N, 7.43, Found: C, 57.58; H, 4.93; N, 7.58.

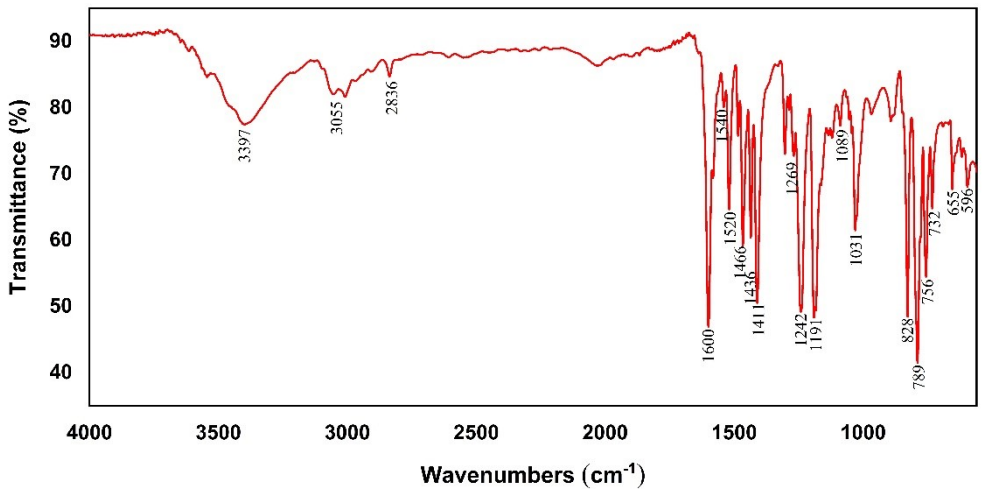

Figure S9 The IR spectrum of complex **9**

[$FeBr_2\mathbf{L}_2^9$] (**9**): IR (KBr, cm^{-1}): 3397 (m, $\upsilon_{O\text{-}H}$), 3055 (m, $\upsilon_{C\text{-}H}$), 2836 (m, $\upsilon_{C\text{-}H}$), 1600 (s, $\upsilon_{C=C}$), 1540 (w, $\upsilon_{C=C}$), 1520 (m, $\upsilon_{C=C}$), 1466 (m, $\delta_{C=C}$), 1436 (m, $\upsilon_{C=C}$), 1411 (s, $\upsilon_{C=C}$), 1269 (w, $\beta_{C\text{-}H}$), 1242 (s, $\upsilon_{C\text{-}O\text{-}C}$), 1191 (s, $\beta_{C\text{-}H}$), 1089 (m, $\beta_{C\text{-}H}$), 1031 (m, $\beta_{C\text{-}H}$), 828 (s, $\gamma_{C\text{-}H}$), 789 (s, $\gamma_{C\text{-}H}$), 756 (s, $\gamma_{C\text{-}H}$), 732 (m, $\gamma_{C\text{-}H}$), 655 (m), 596 (m). Elemental analysis: Anal. calcd for $C_{44}H_{34}O_2N_6Br_2Fe\cdot 5H_2O$:C, 53.68; H, 4.50; N, 8.54, Found: C, 53.47; H,4.45; N, 8.47.

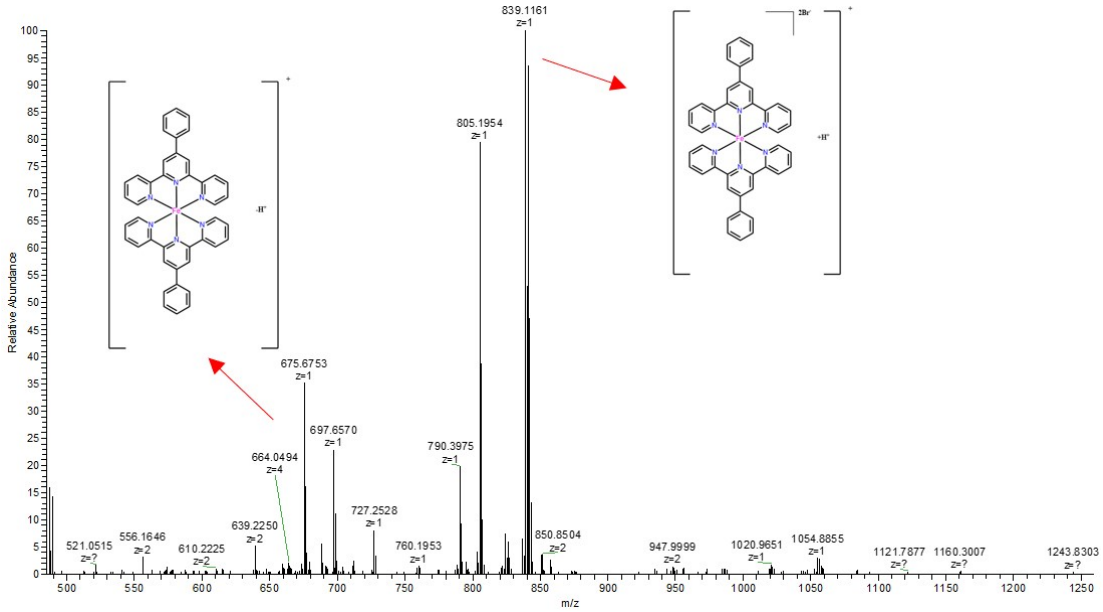

Figure S10 The ESI-MS spectrum of complex **1**

(ESI-MS: [$Fe\mathbf{L}_2^1$ - H^+]$^+$: 675.6753, [$FeBr_2\mathbf{L}_2^1$ + H^+]$^+$: 839.1161)

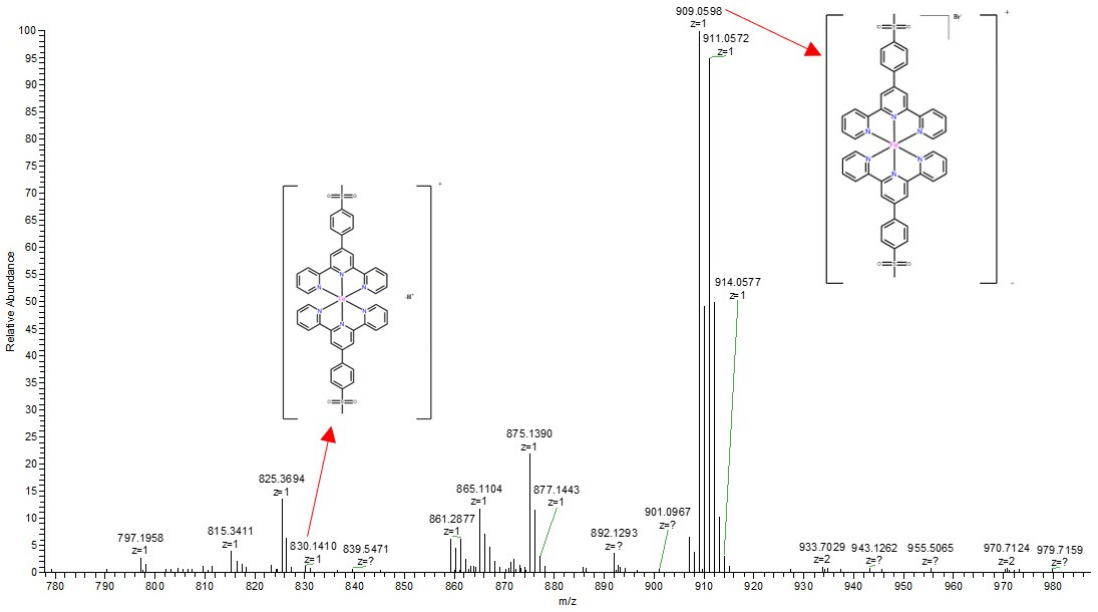

Figure S11 The ESI-MS spectrum of complex **2**

(ESI-MS: $[FeL_2^2 - H^+]^+$: 830.1410, $[FeBrL_2^2]^+$: 909.0598)

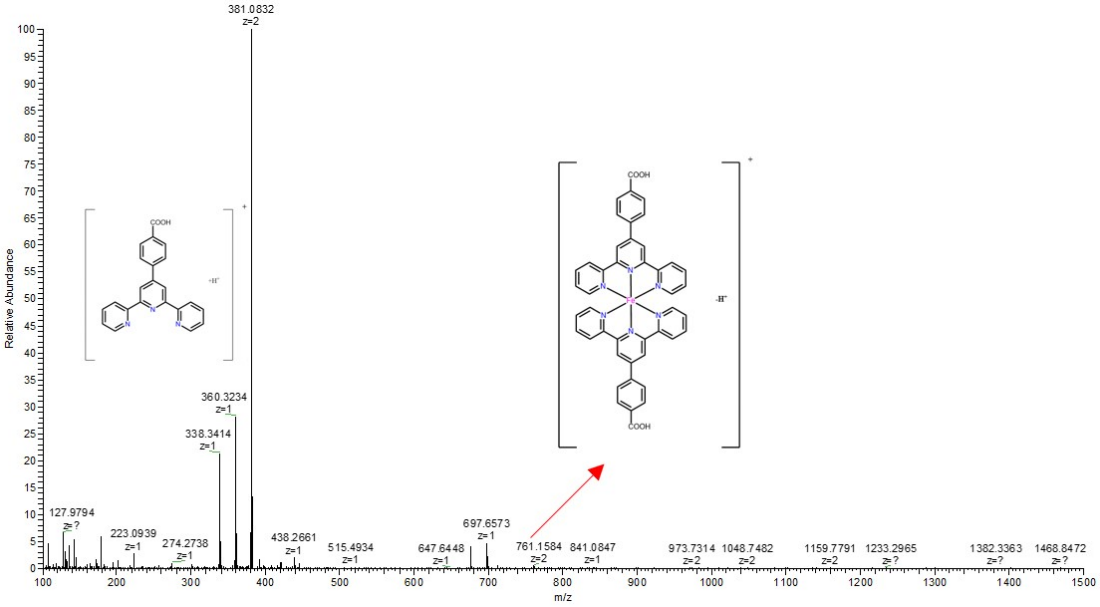

Figure S12 The ESI-MS spectrum of complex **3**

(ESI-MS: $[L_1^3 + H^+]^+$: 360.3234, $[FeL_2^3 - H^+]^+$: 761.1584)

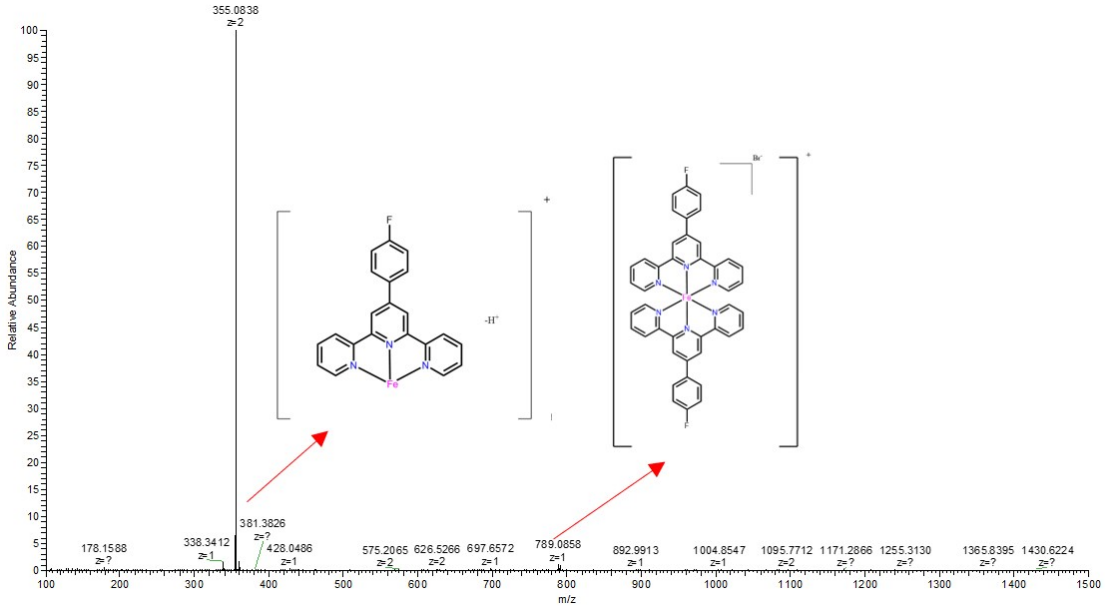

Figure S13 The ESI-MS spectrum of complex **4**

(ESI-MS: $[Fe\mathbf{L}_1{}^4 - H^+]^+$: 381.3826, $[FeBr\mathbf{L}_2{}^4]^+$: 789.0858)

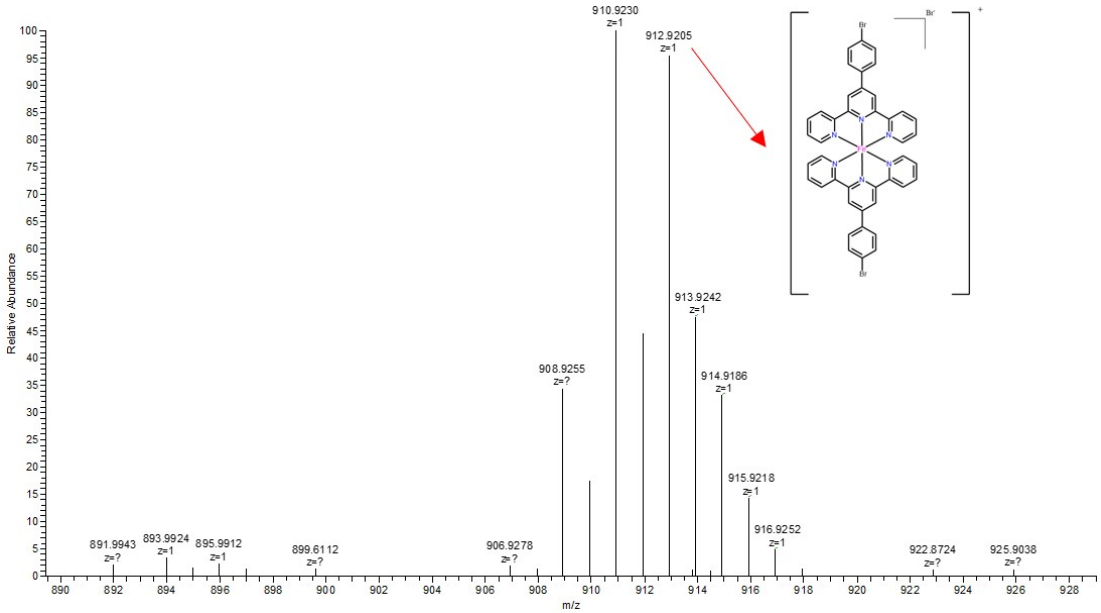

Figure S14 The ESI-MS spectrum of complex **5**

(ESI-MS: $[FeBr\mathbf{L}_2{}^5]^+$: 912.9205)

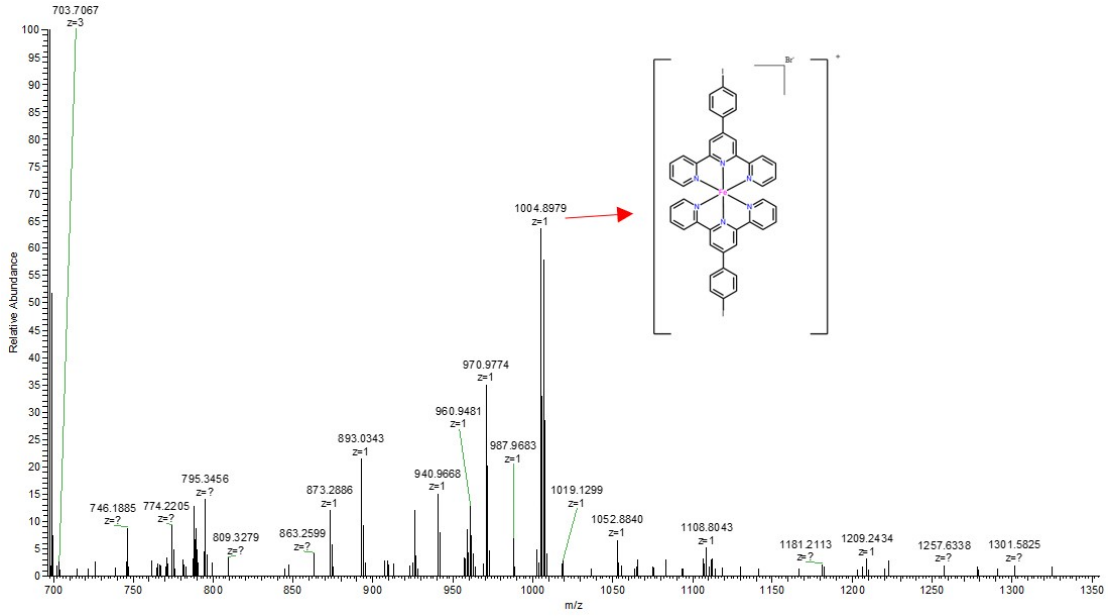

Figure S15 The ESI-MS spectrum of complex **6**

(ESI-MS: $[FeBr\mathbf{L}_2{}^6]^+$: 1004.8979)

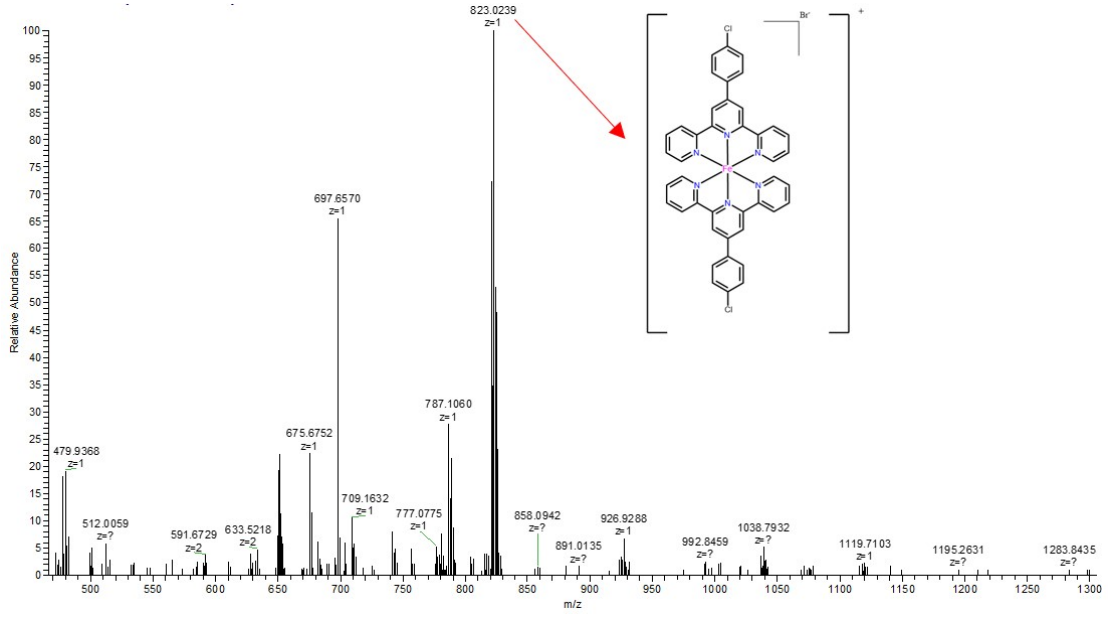

Figure S16 The ESI-MS spectrum of complex **7**

(ESI-MS: $[FeBr\mathbf{L}_2{}^7]^+$: 823.0239)

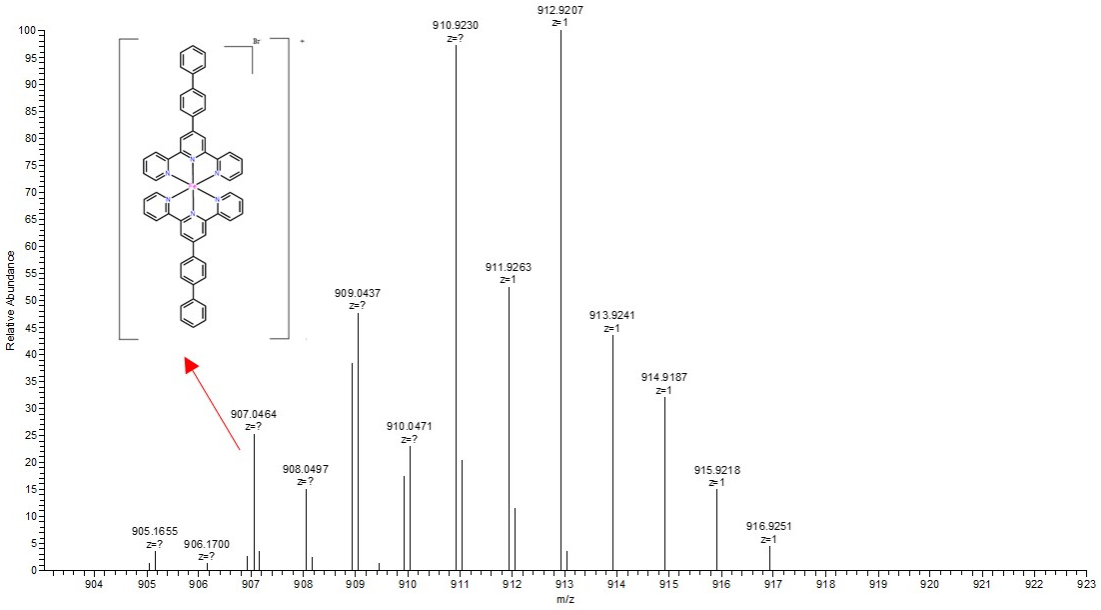

Figure S17 The ESI-MS spectrum of complex **8**

(ESI-MS: $[FeBr\mathbf{L}_2{}^{8}]^+$: 907.0464)

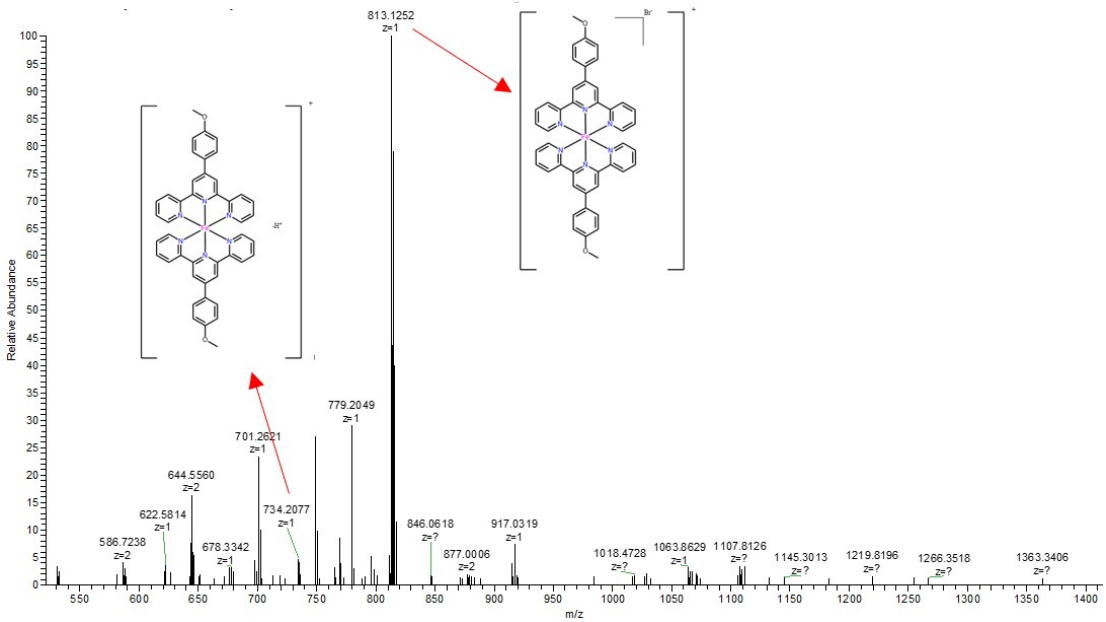

Figure S18 The ESI-MS spectrum of complex **9**

(ESI-MS: $[Fe\mathbf{L}_1{}^{9} - H^+]^+$: 734.2077, $[FeBr\mathbf{L}_2{}^{9}]^+$: 813.1252)

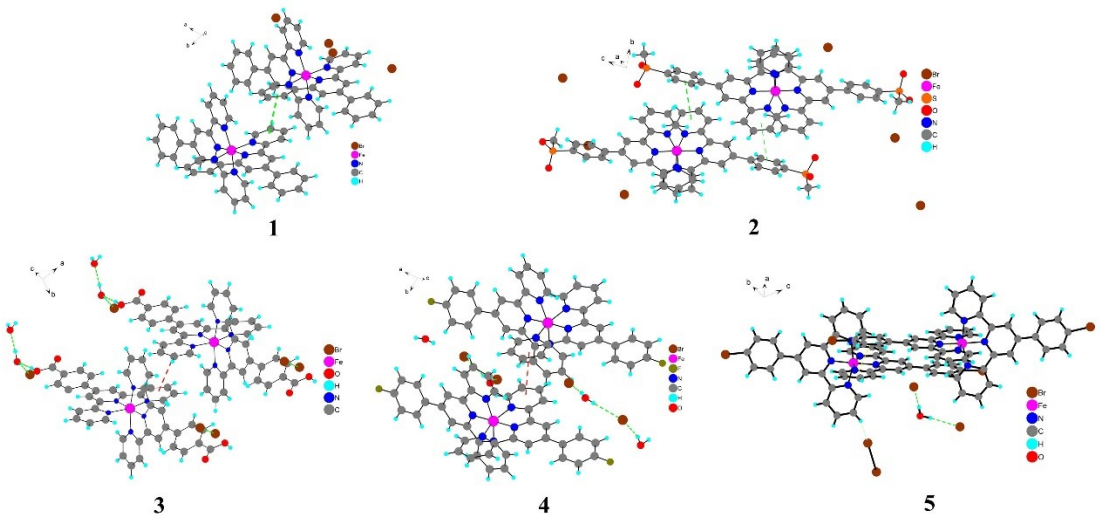

Figure S19 Stacking diagram of complexes **1-5** structure

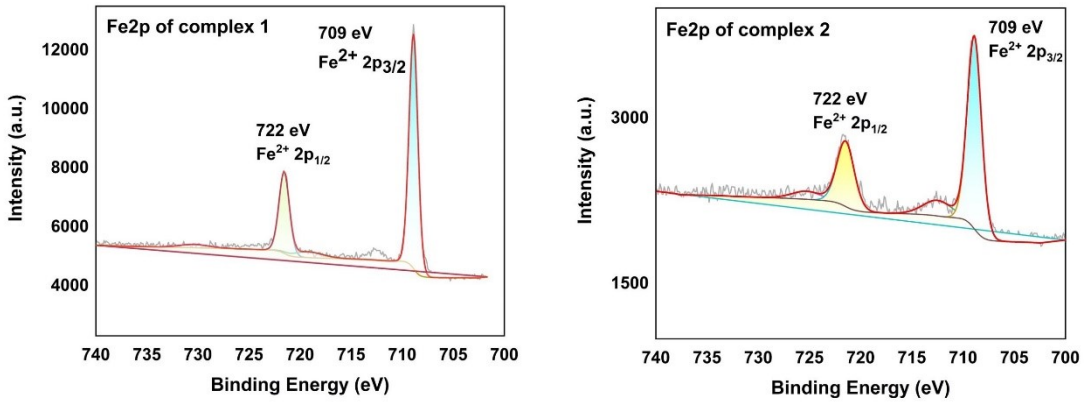

Figure S20 Fe2p XPS spectra of complexes **1-2**

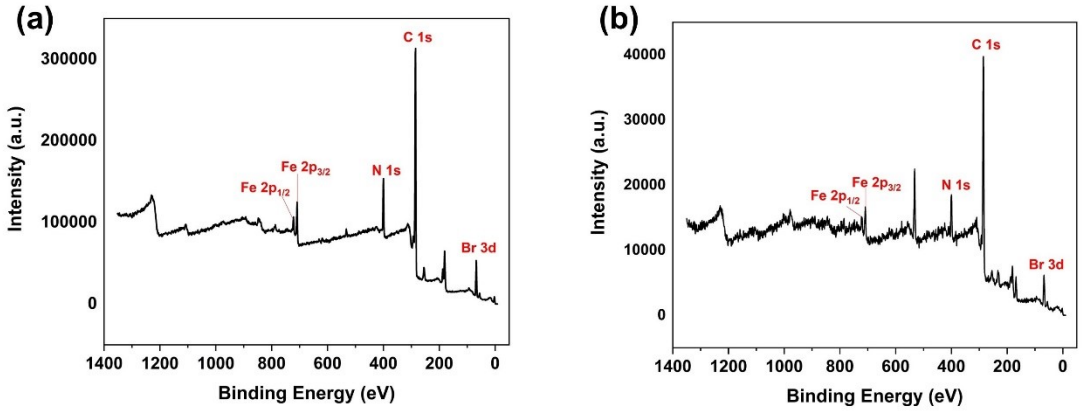

Figure S21 XPS survey scan of complexes **1**(a) and **2**(b)

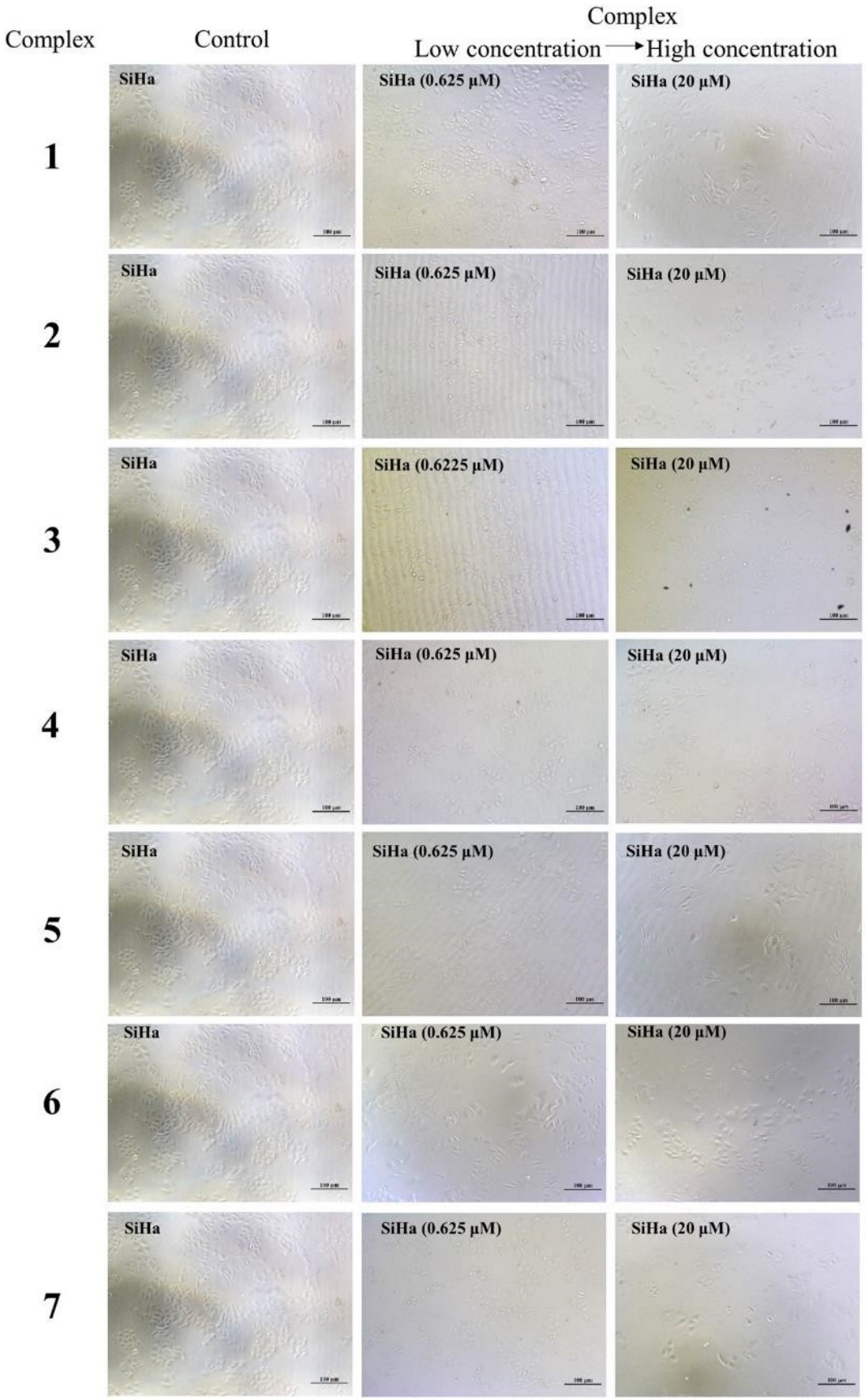
Complex
Control
Complex
Low concentration → High concentration
1
SiHa
SiHa (0.625 µM)
SiHa (20 µM)
2
SiHa
SiHa (0.625 µM)
SiHa (20 µM)
3
SiHa
SiHa (0.6225 µM)
SiHa (20 µM)
4
SiHa
SiHa (0.625 µM)
SiHa (20 µM)
5
SiHa
SiHa (0.625 µM)
SiHa (20 µM)
6
SiHa
SiHa (0.625 µM)
SiHa (20 µM)
7
SiHa
SiHa (0.625 µM)
SiHa (20 µM)

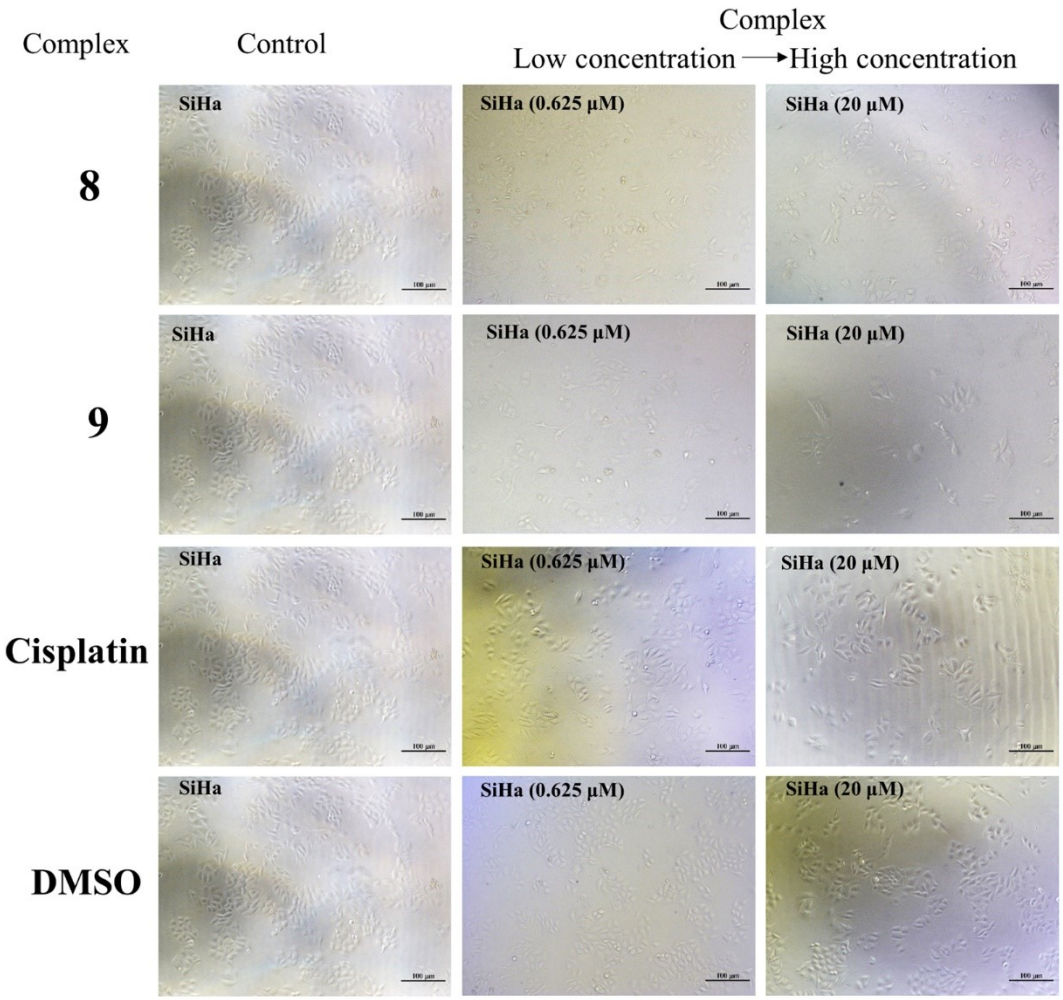

Figure. S22 The microscopic images of SiHa cells after treating with complexes **1-9** and cisplatin

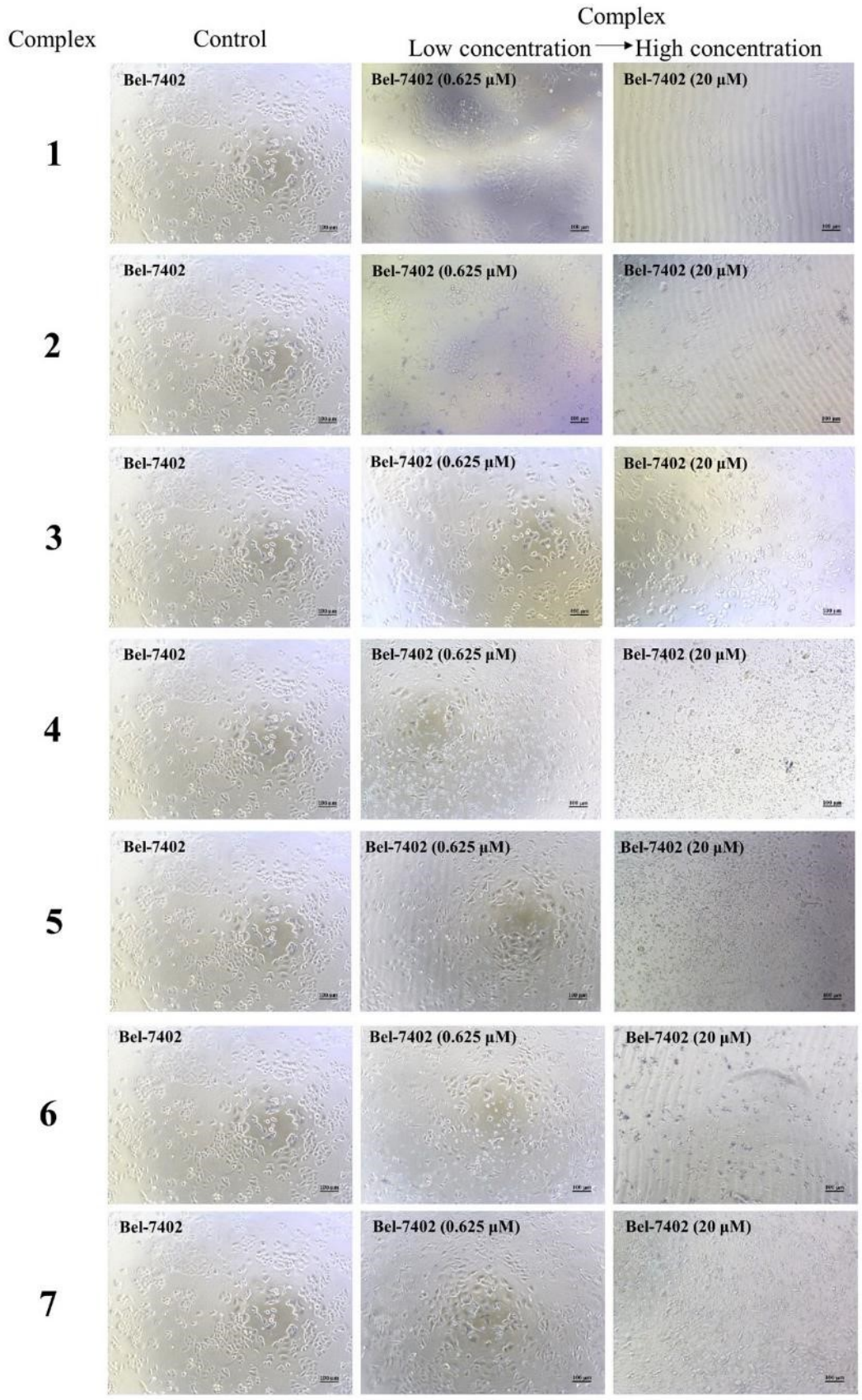
Complex
Control
Complex
Low concentration → High concentration
1
2
3
4
5
6
7
Bel-7402
Bel-7402 (0.625 μM)
Bel-7402 (20 μM)

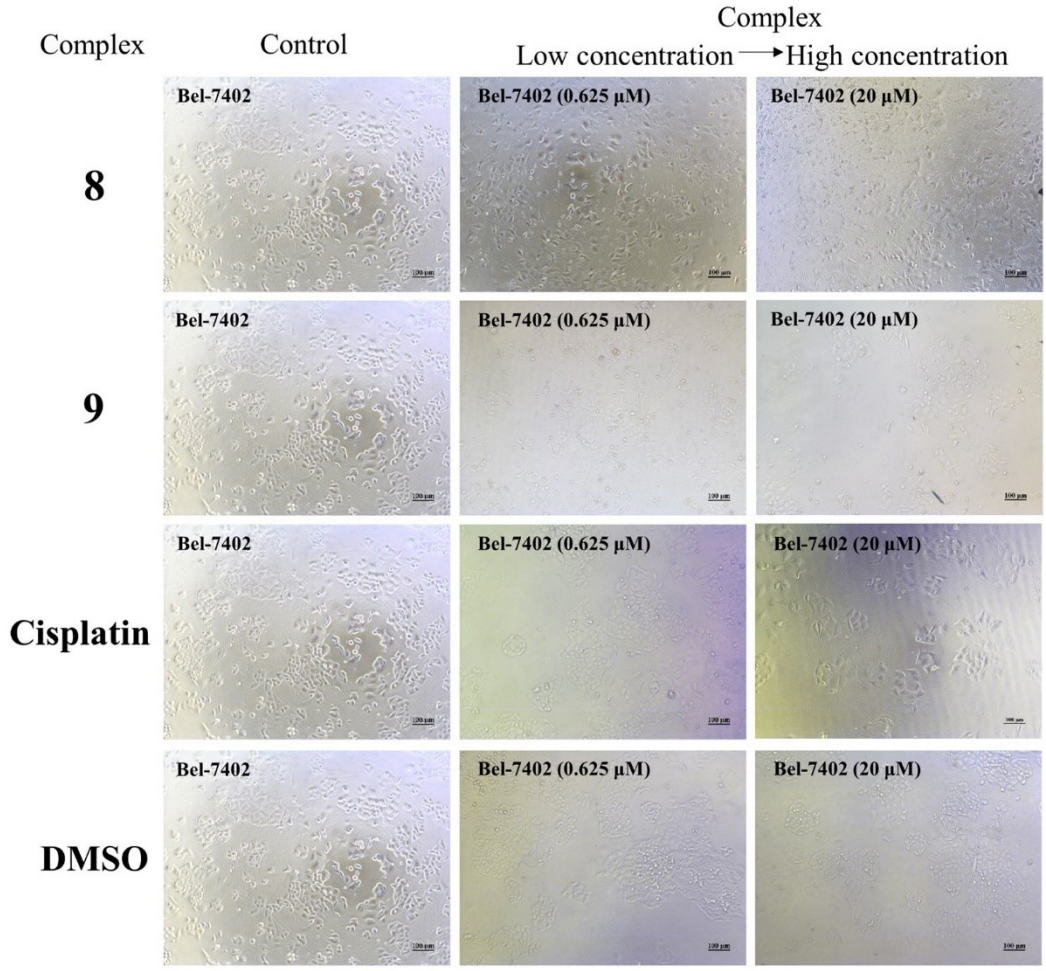

Figure. S23 The microscopic images of Bel-7402 cells after treating with complexes **1-9** and cisplatin

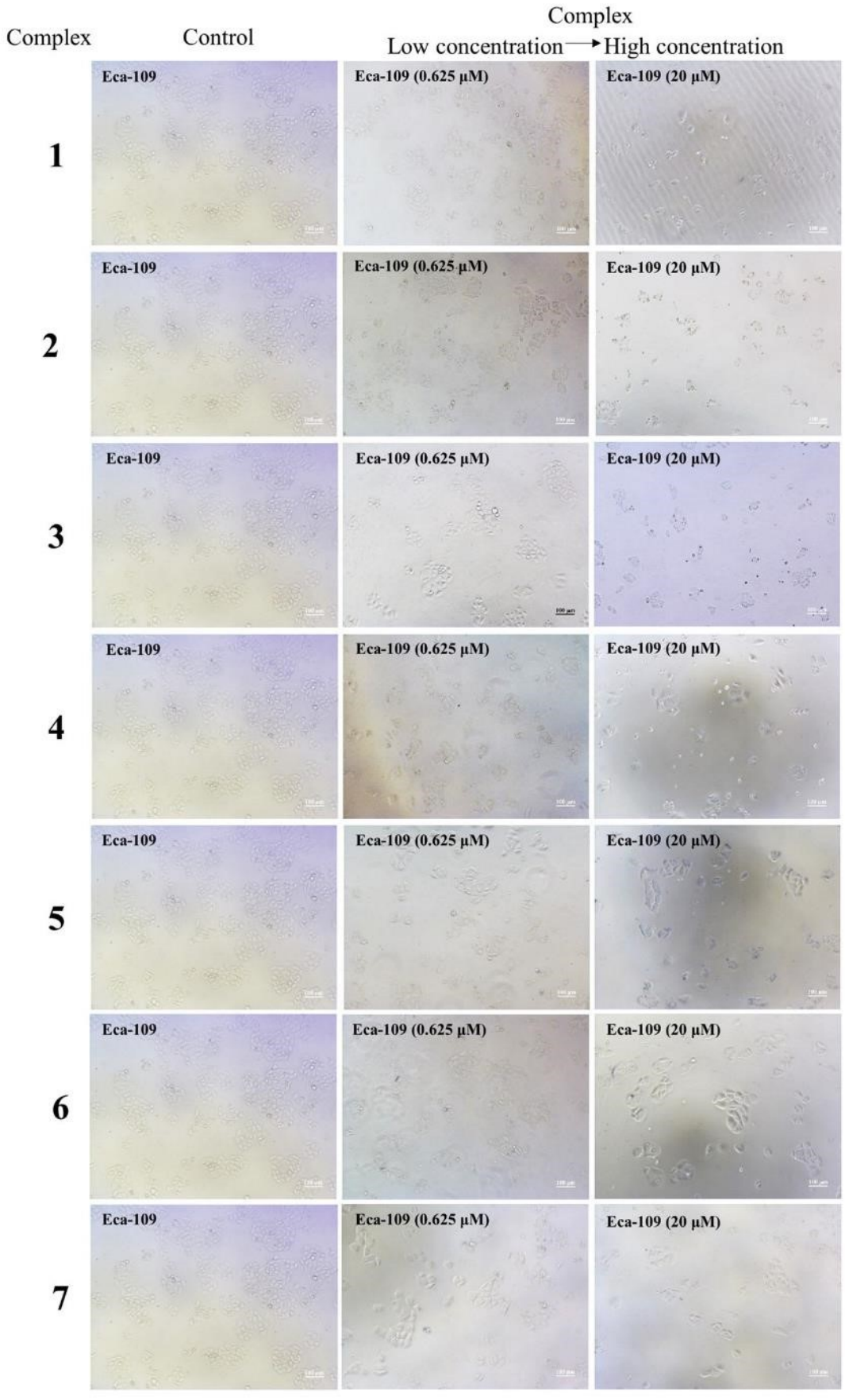
Complex
Control
Complex
Low concentration → High concentration
1
2
3
4
5
6
7
Eca-109
Eca-109 (0.625 μM)
Eca-109 (20 μM)

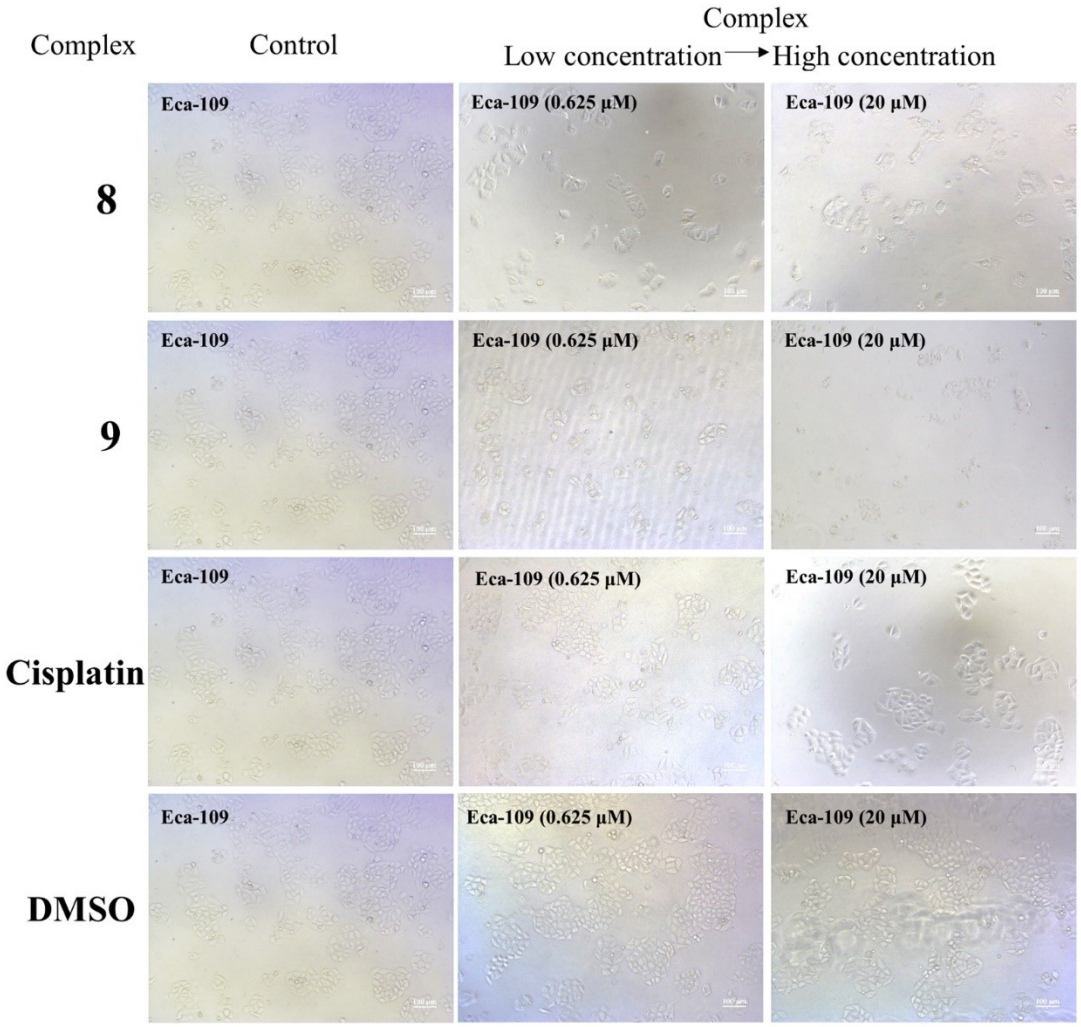

Figure. S24 The microscopic images of Eca-109 cells after treating with complexes **1-9** and cisplatin

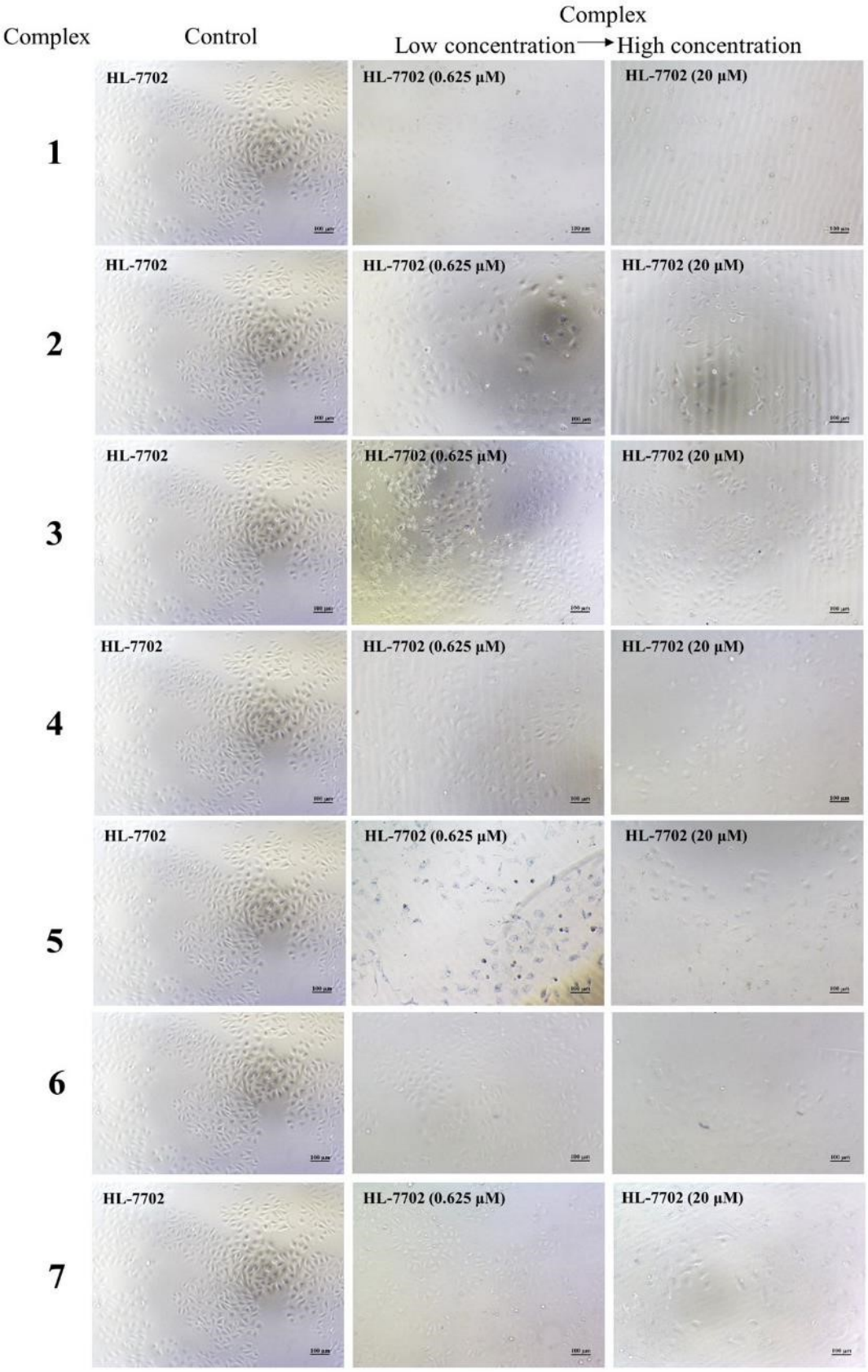
Complex
Control
Complex
Low concentration → High concentration
1
2
3
4
5
6
7
HL-7702
HL-7702 (0.625 μM)
HL-7702 (20 μM)

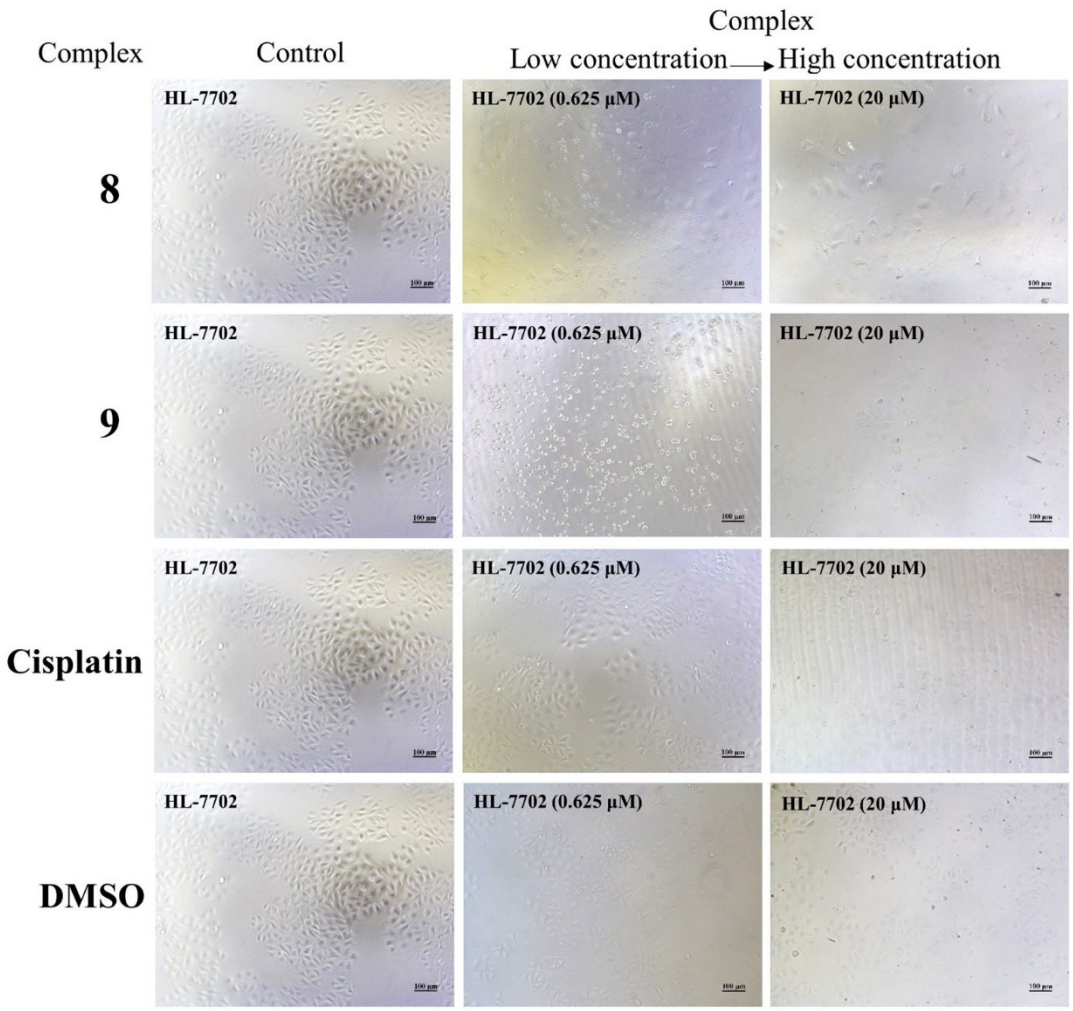

Figure. S25 The microscopic images of HL-7702 cells after treating with complexes **1-9** and cisplatin

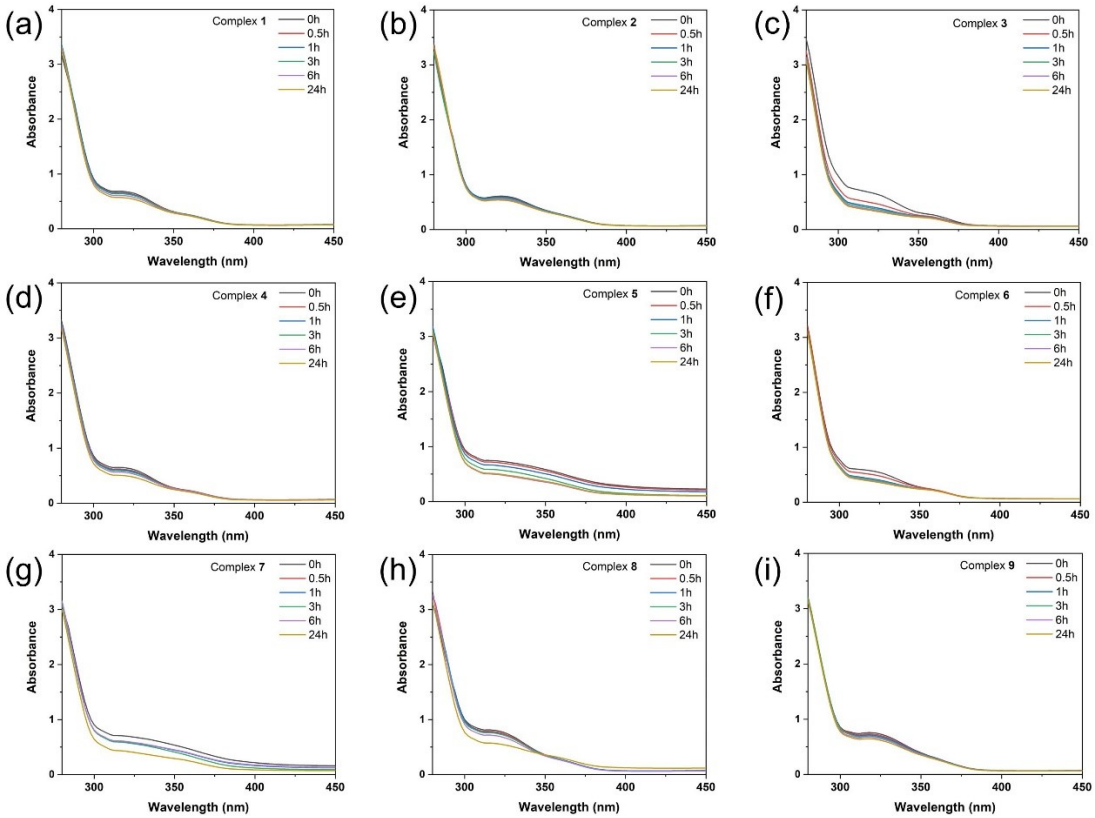

Figure. S26 UV spectra of complexes **1-9** in Tris-HCl buffer (pH 7.2) recorded at different times (within 24 h) at room temperature

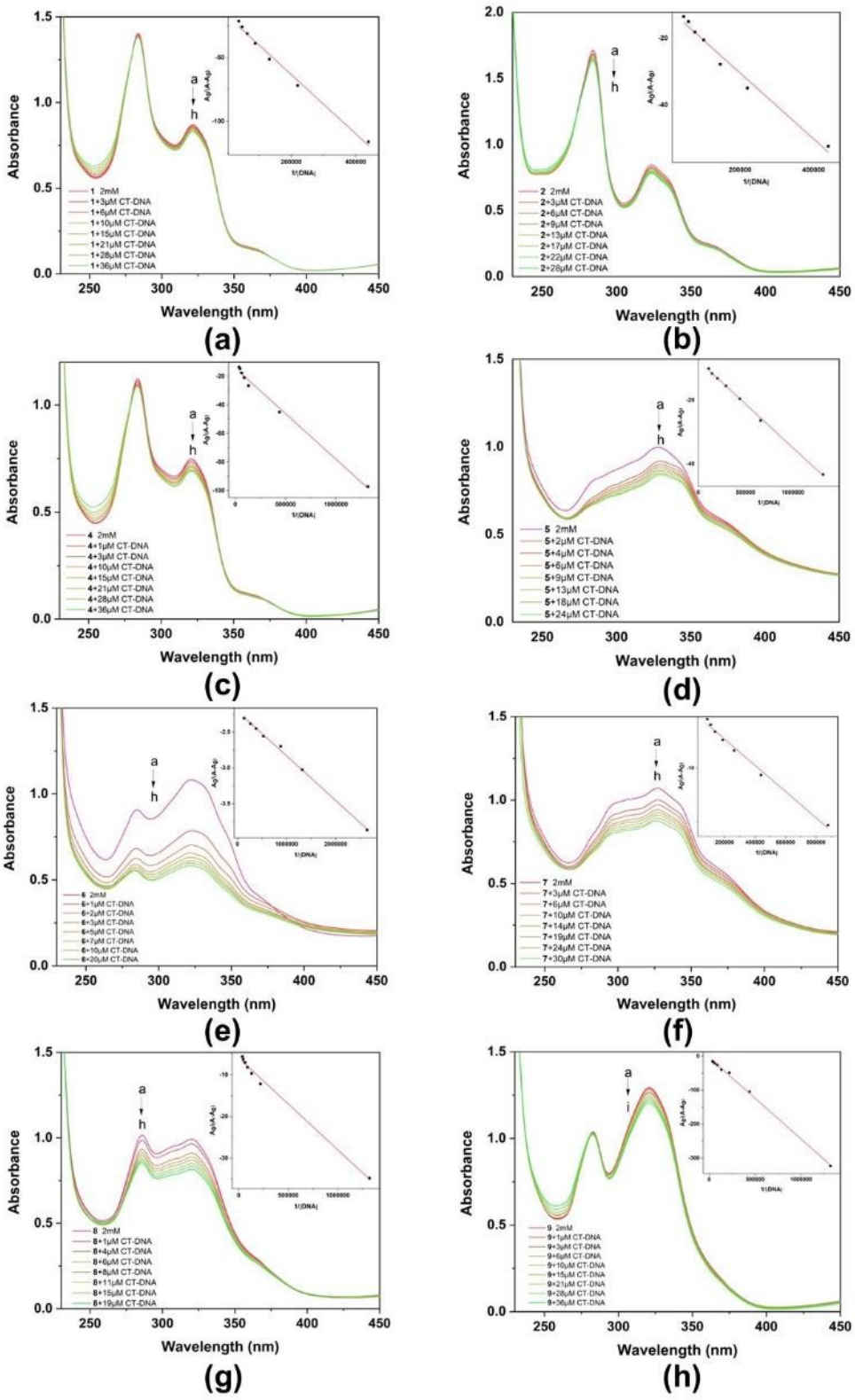

Figure S27 Absorption spectra of 15 μM of complexes **1-2**(a-b) and **4-9**(c-h) in a Tris-HCl buffer (pH = 7.2) solution with series concentrations of CT-DNA. The plots of $A_0/(A-A_0)$ versus the concentration of CT-DNA are shown as the insets

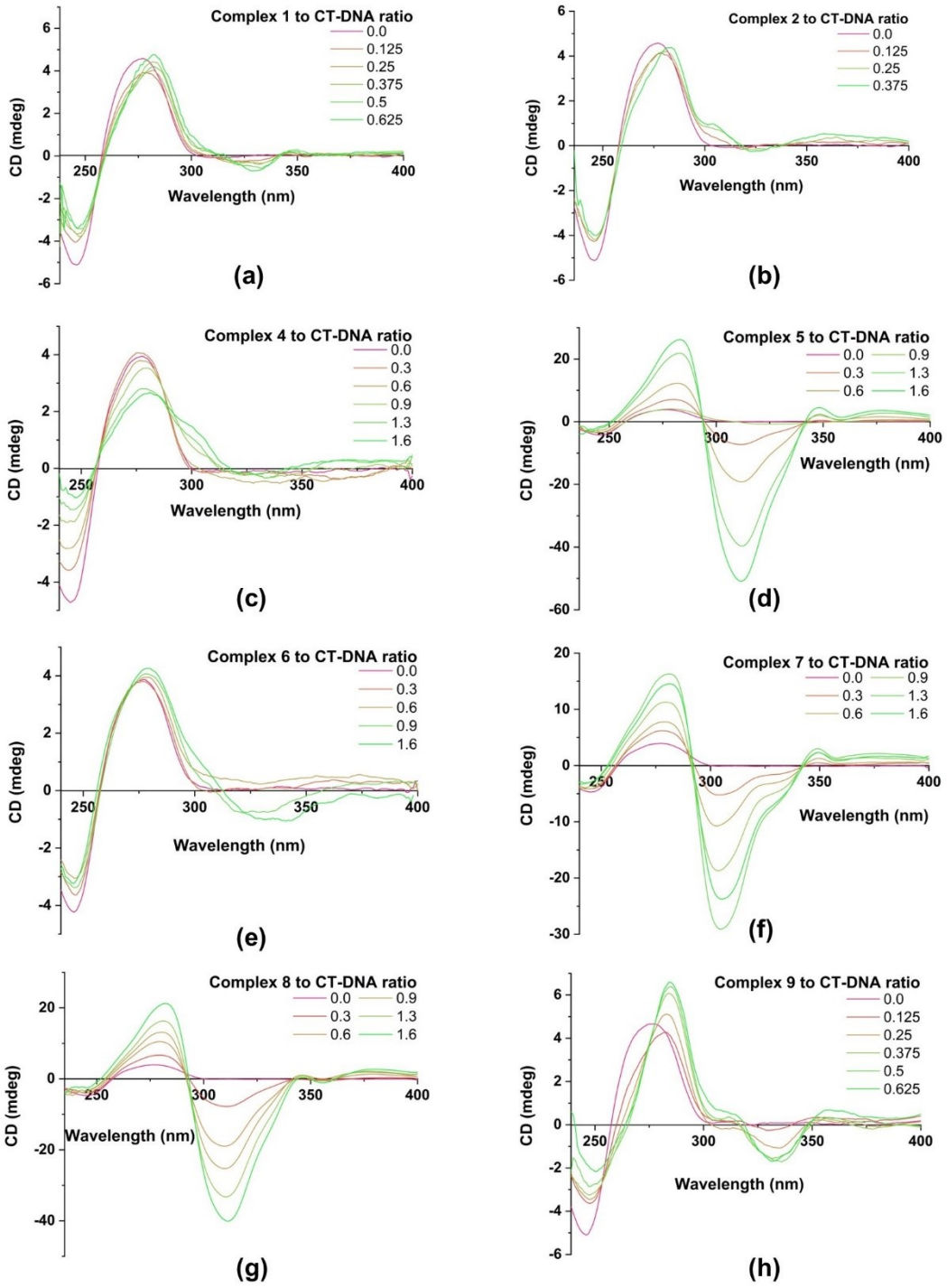

Figure S28 CD spectra of complexes **1-2**(a-b) and **4-9**(c-h) to CT-DNA at different concentration ratios

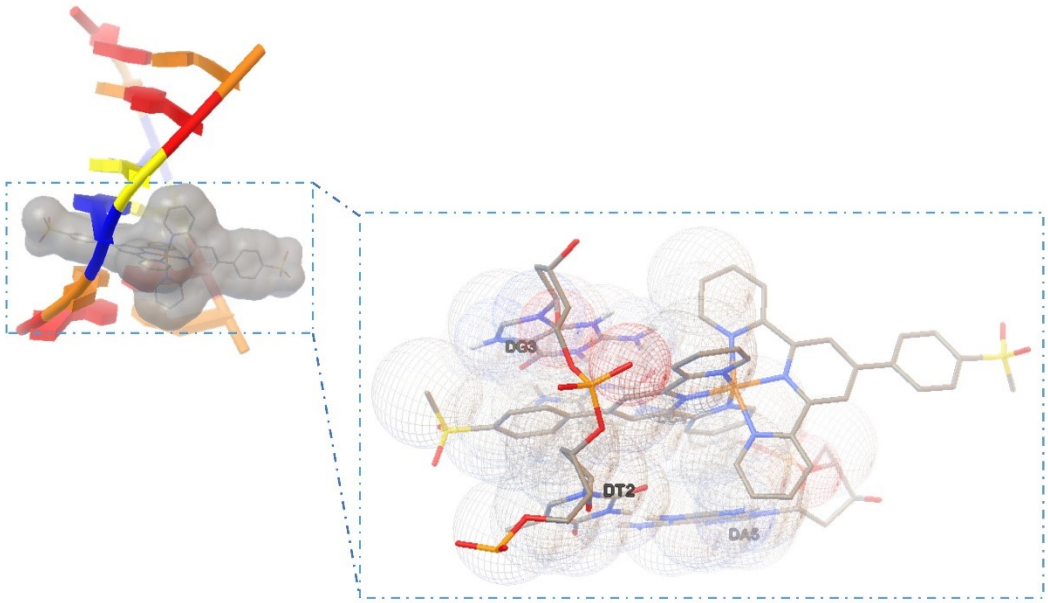

Figure S29 The most favorable conformation of complex **2** bound with oligonucleotide (4JD8)

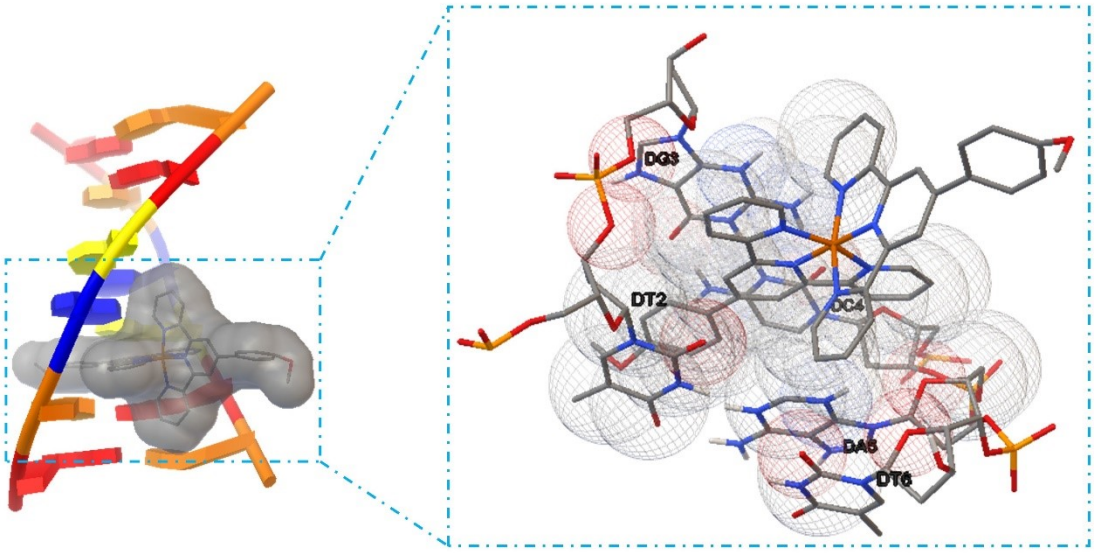

Figure S30 The most favorable conformation of complex **3** bound with oligonucleotide (4JD8)

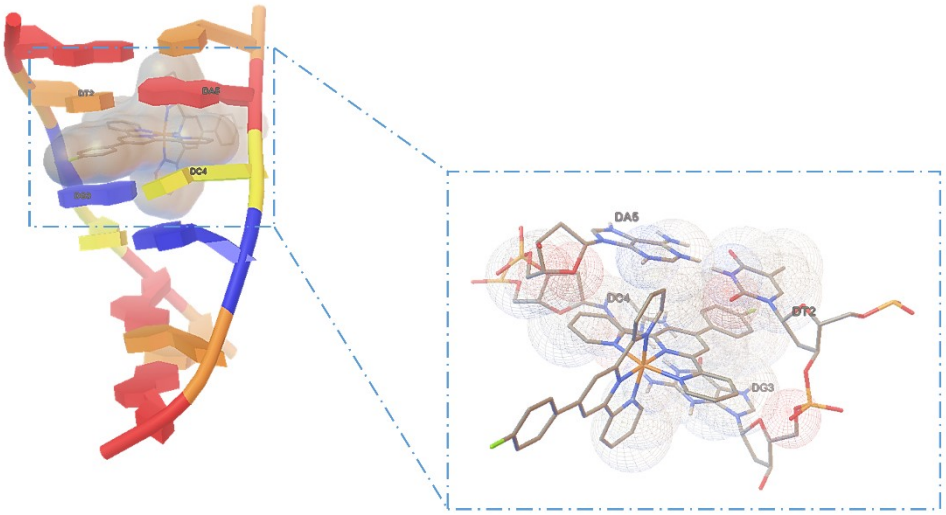

Figure S31 The most favorable conformation of complex **4** bound with oligonucleotide (4JD8)

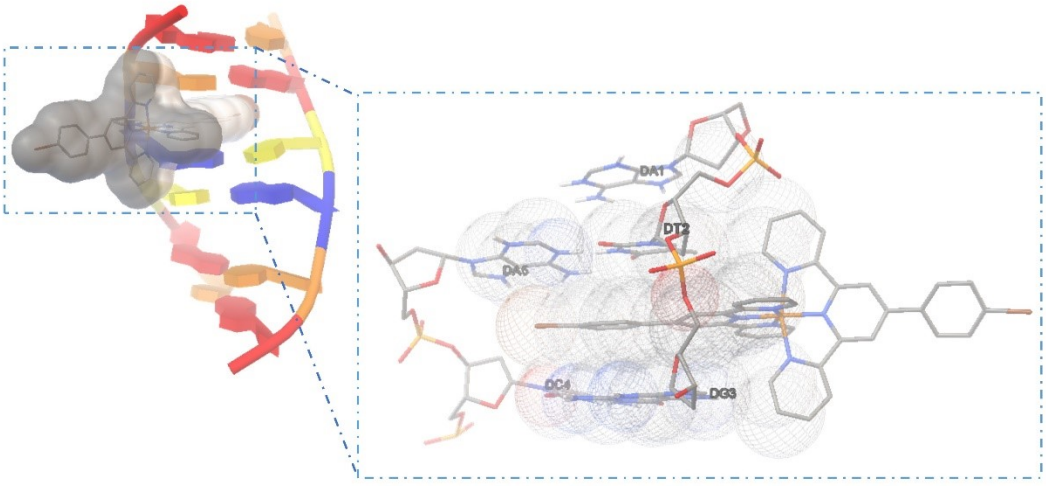

Figure S32 The most favorable conformation of complex **5** bound with oligonucleotide (4JD8)

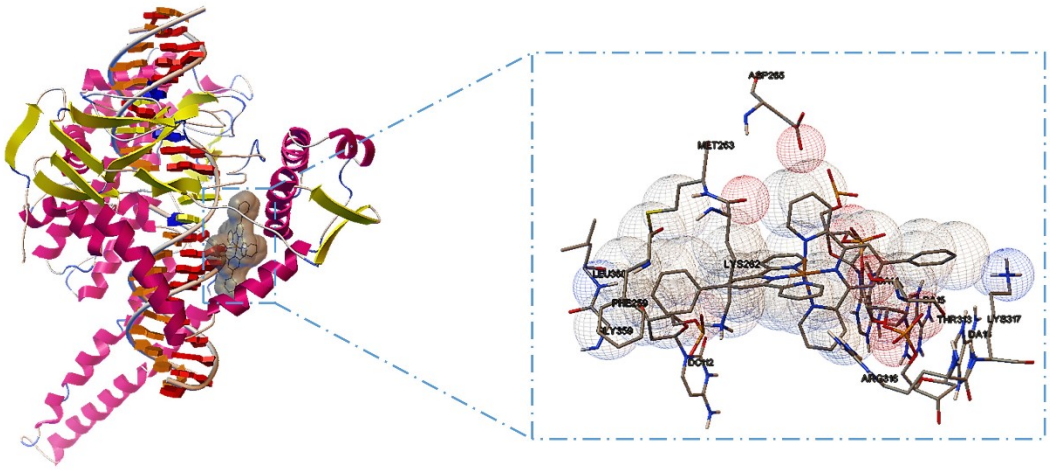

Figure S33 The most favorable conformation of complex **1** bound with DNA-Topo I (1SC7)

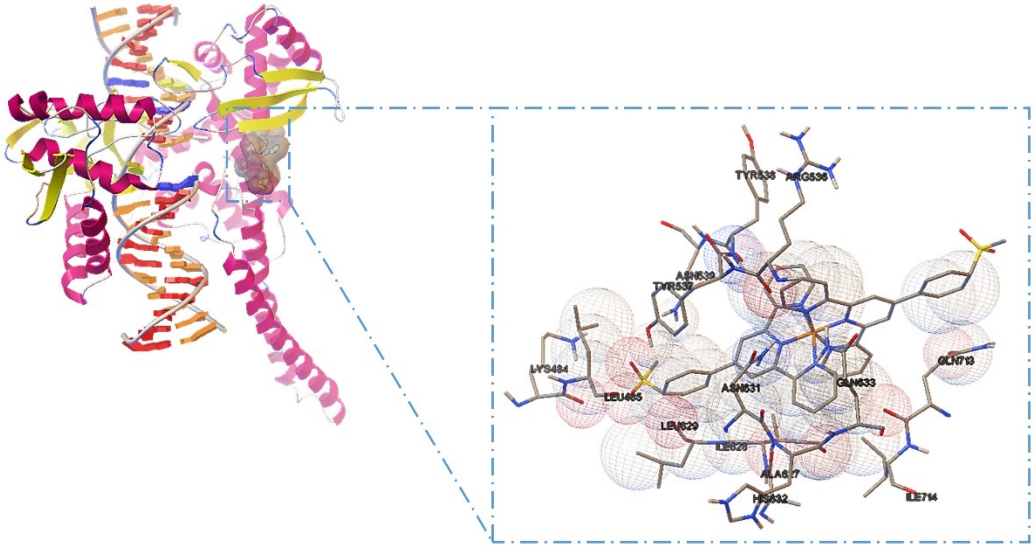

Figure S34 The most favorable conformation of complex **2** bound with DNA-Topo I (1SC7)

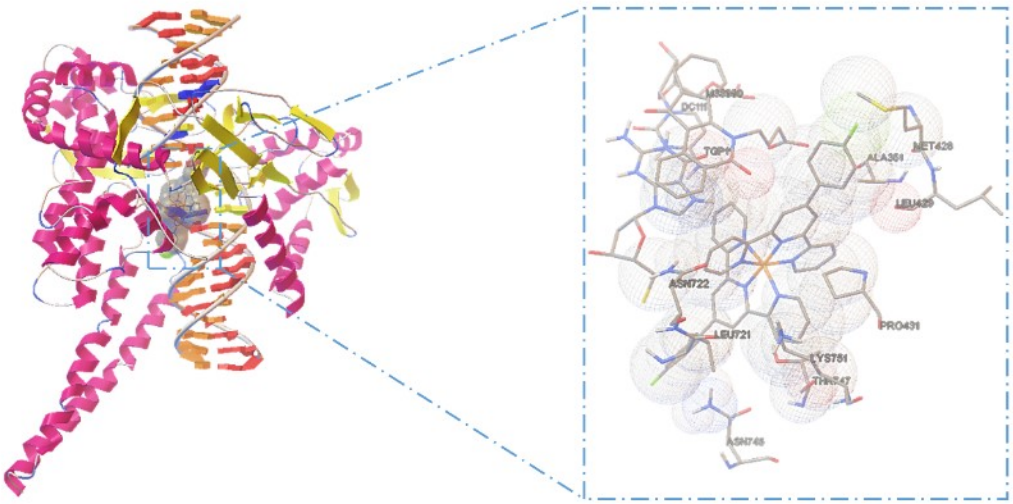

Figure S35 The most favorable conformation of complex **4** bound with DNA-Topo I (1SC7)

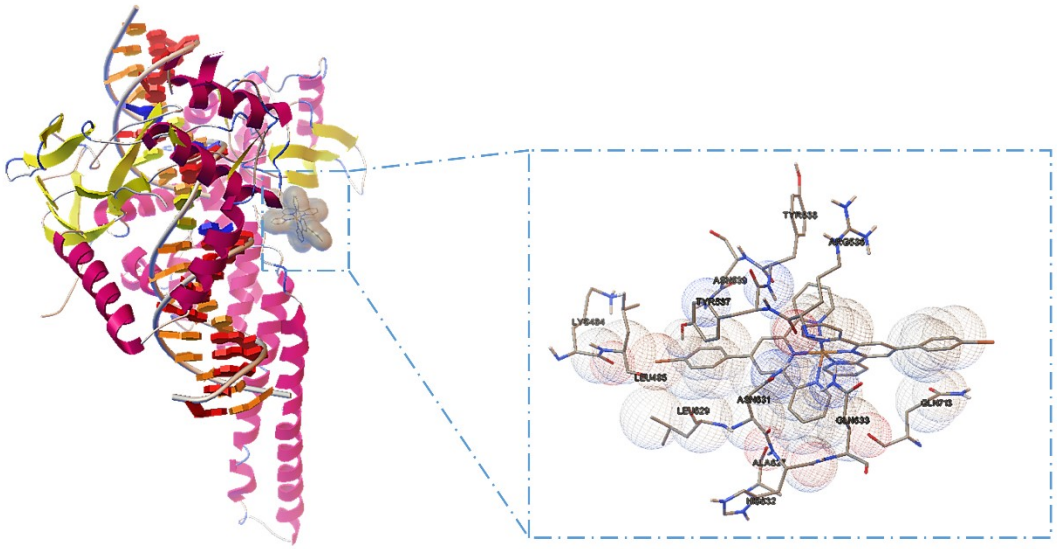

Figure S36 The most favorable conformation of complex **5** bound with DNA-Topo I (1SC7)

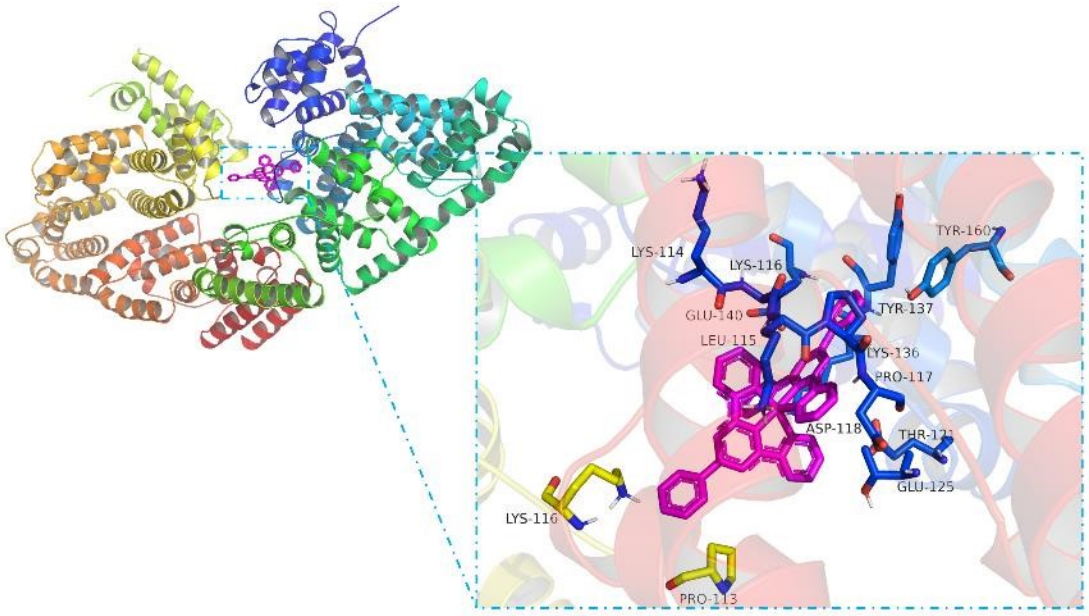

Figure S37 The most favorable conformation of complex **1** bound with BSA (4F5S)

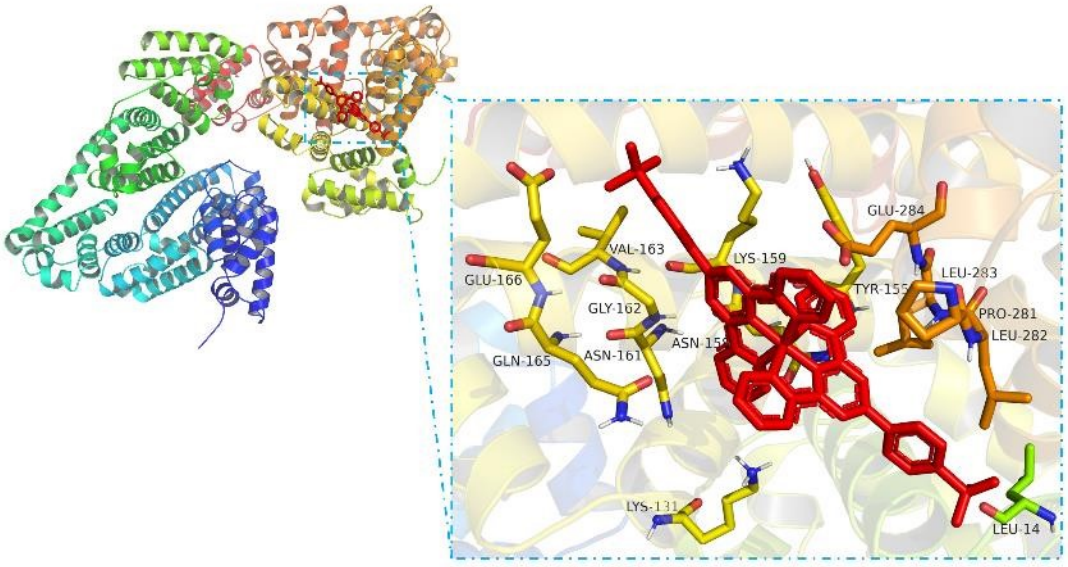

Figure S38 The most favorable conformation of complex **2** bound with BSA (4F5S)

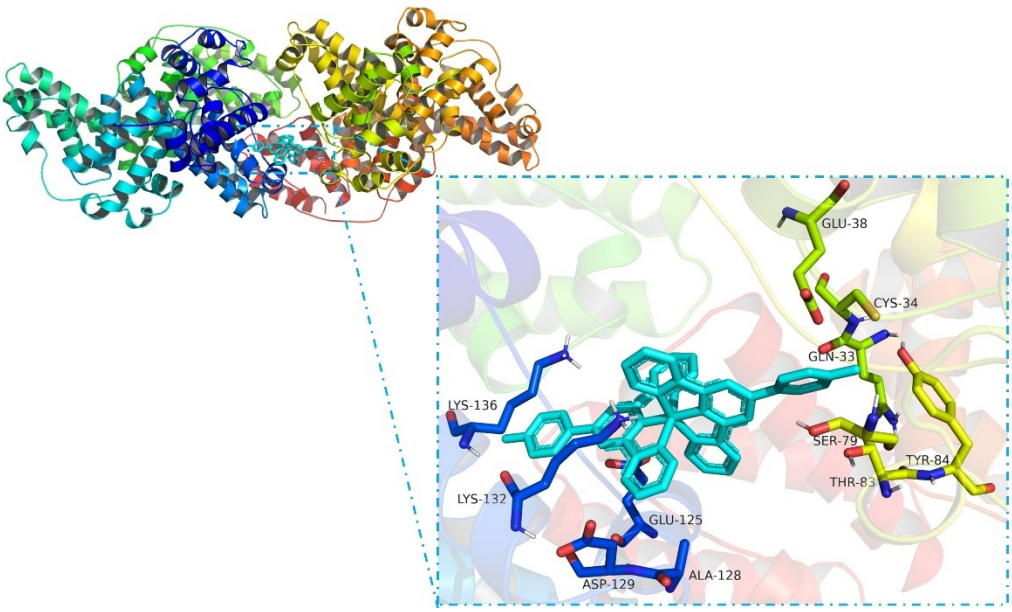

Figure S39 The most favorable conformation of complex **4** bound with BSA (4F5S)

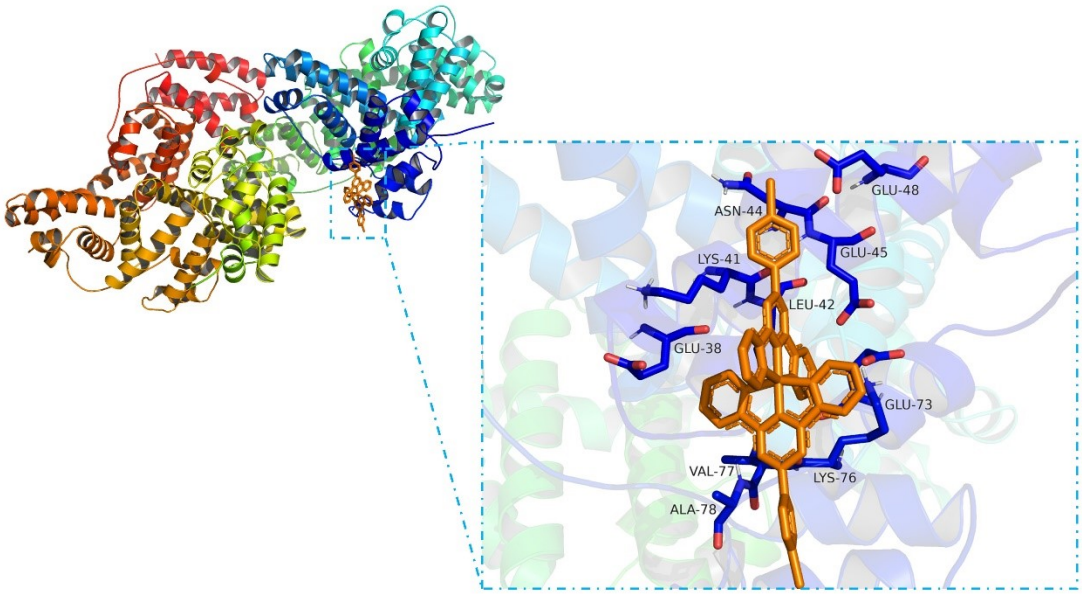

Figure S40 The most favorable conformation of complex **5** bound with BSA (4F5S)

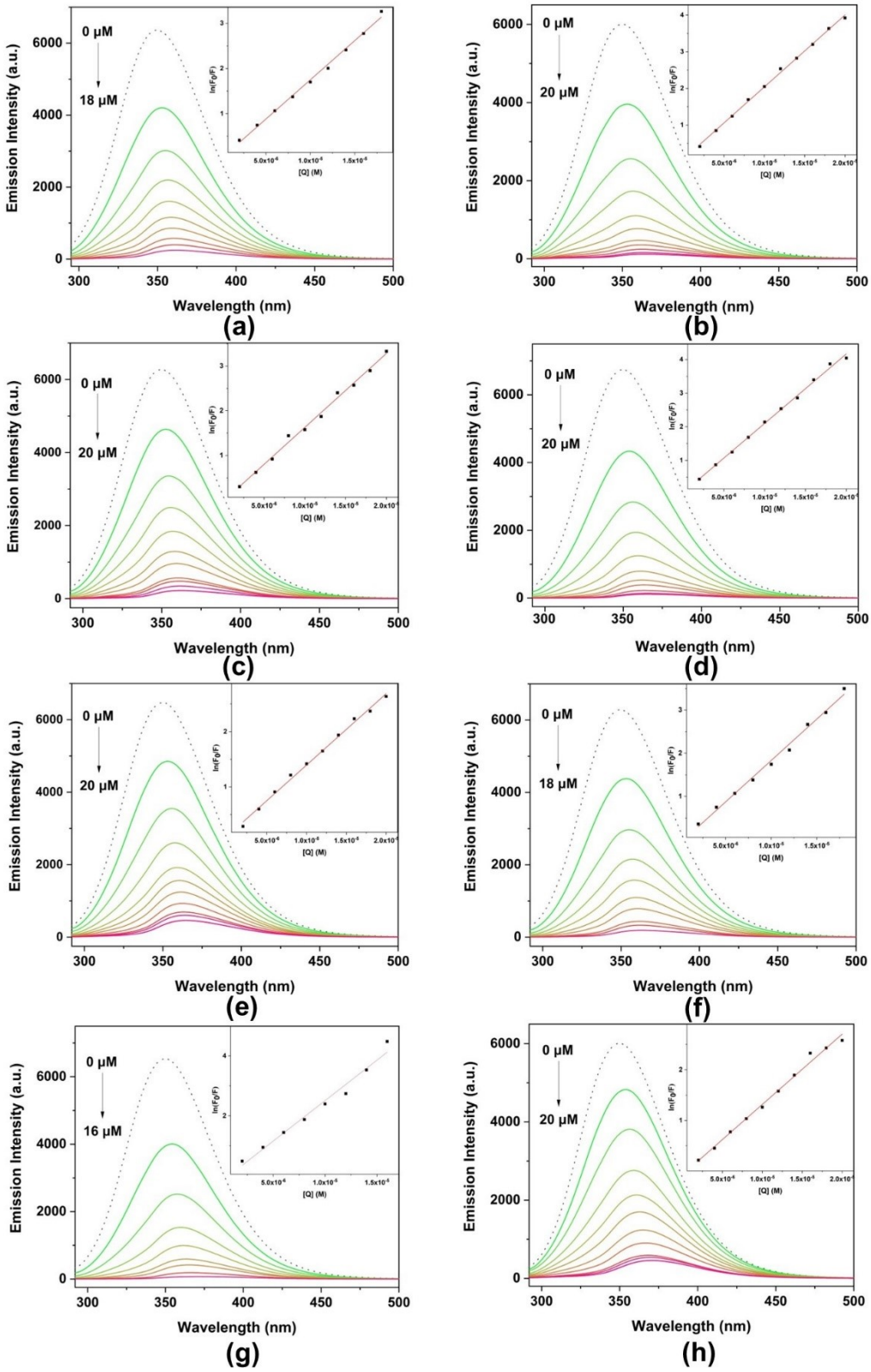

Figure S41 Fluorescence spectra of 20 μM BSA in the absence (dotted line) and presence (2-20 μM) of complexes **1-2**(a-b) and **4-9**(c-h) (solid line)

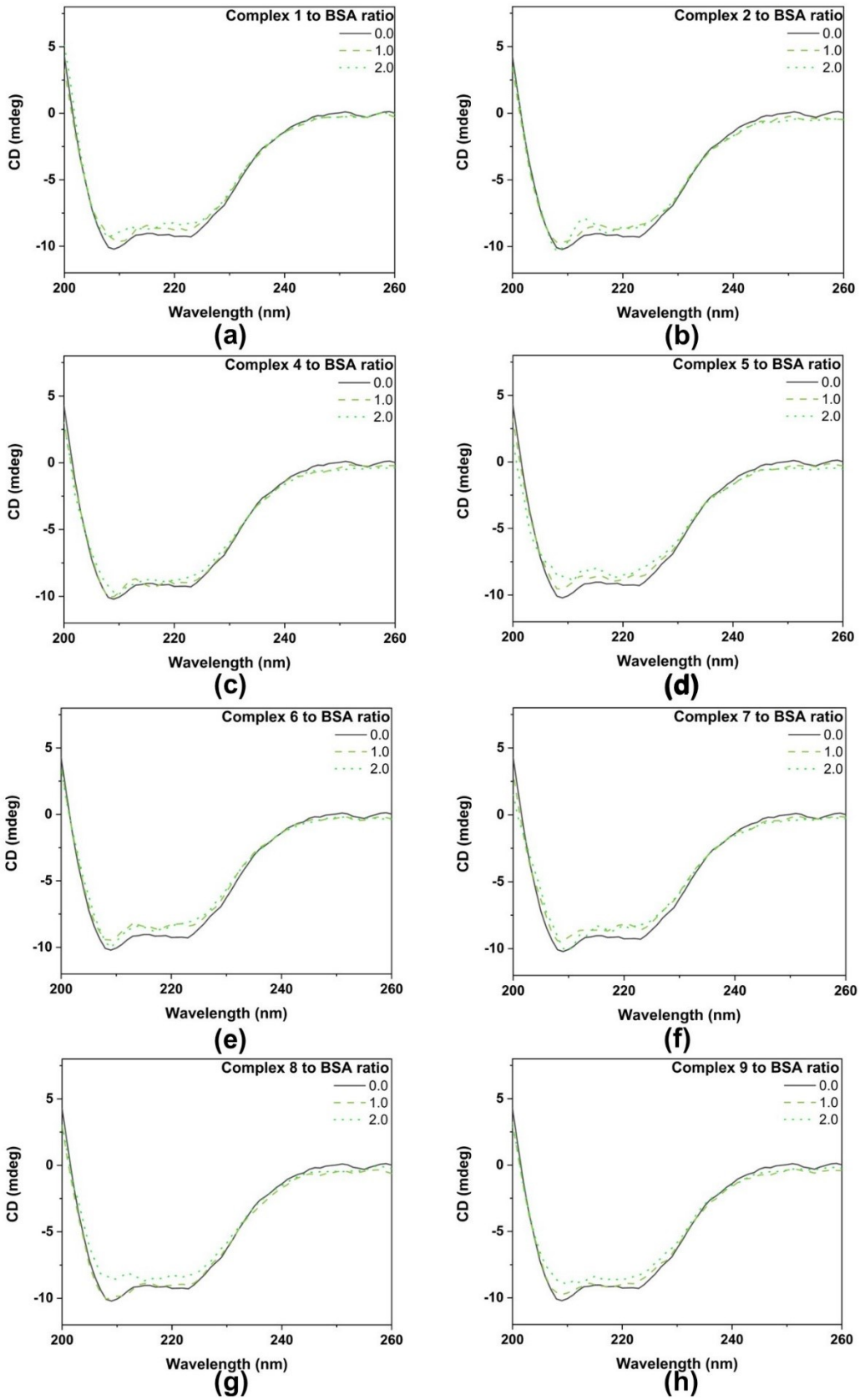

Figure S42 CD spectra of complexes **1-2**(a-b) and **4-9**(c-h) to BSA at different concentration ratios

Table S1 Percentage of element content measured in XPS

Name	Atomic % (complex **1**)	Atomic % (complex **2**)
C 1s	93.07	93.21
Fe 2p	2.15	2.49
Br 3d	4.79	4.29